Whole Ecosystem Measurements of Biogenic Hydrocarbon Emissions

Final Report

ARB Award No. 98-328

STATE OF CALIFORNIA AIR RESOURCES BOARD

Principal Investigator

Dr. Allen H. Goldstein

Department of Environmental Science, Policy, and Management
Ecosystem Sciences Division
151 Hilgard Hall
University of California
Berkeley, CA 94720-3110
(510)643-2451
ahg@nature.berkeley.edu

Co-Investigator

Dr. Gunnar W. Schade

Department of Environmental Science, Policy, and Mangement
Ecosystem Sciences Division
151 Hilgard Hall
University of California
Berkeley, CA 94720-3110
(510)643-6449
gws@nature.berkeley.edu

Contributing Researcher

Gabrielle Dreyfus

May 15, 2001

ACKNOWLEDGEMENTS

Several individuals from the California Air Resources Board contributed to this project. We specially want to thank Ash Lashgari and Michael Benjamin for their steadfast encouragement and useful input throughout the contract period.

The success of this study depended on the work of many individuals. In particular, several members of the Goldstein research group at UC Berkeley worked very hard to maintain the research site and collect data on ecosystem scale biosphere-atmosphere fluxes of trace gases and energy at the Blodgett Forest Tower Site, and on the physical structure and physiological functioning of the ecosystem. For these efforts we particularly thank Nathan Hultman, Meredith Kurpius, Megan McKay, and Jeanne Panek. We also thank Marcus Lamanna for his earlier work in building the automated in-situ gas chromatograph system for measuring volatile organic compound mixing ratios. Other researchers who deserve thanks for their substantial contributions to the related research on biosphere-atmosphere exchange and regional photochemistry at Blodgett Forest included Ronald Cohen, Michael Dillon, Douglas Day, Dennis Gray, Judith Charles, Reggie Spaulding, Melissa Lunden, Doug Black, Ye Qi, and Ming Xu. We also thank Dave Bowling for valuable input on development of the Relaxed Eddy Accumulation system.

The staff at Blodgett forest was instrumental to the success of this project. We are particularly indebted to Bob Heald, Dave Rambeau, Sheryl Rambeau, Tony Sargenti, and Frieder Schurr for their extensive participation in keeping the field site operational and accessible. We also thank Sierra Pacific Industries for allowing us to carry out this research on their property.

We gratefully acknowledge support for this research by the California Air Resources Board (award 98-328). Additional support that was used to maintain the related ongoing research projects at the Blodgett Forest Tower Site included funding from the U.S. Department of Energy (contract DE-AC03-76SF0009), the Environmental Protection Agency STAR Ecosystem Indicators Program (award R826601), and the University of California Agricultural Experiment Station. G. Schade acknowledges funding from the German Academic Exchange Service during year one of this contract.

TABLE OF CONTENTS

LIST OF TABLES

LIST OF FIGURES

EXECUTIVE SUMMARY

Over the past few decades it has become well established that emissions of volatile organic compounds (VOC) from vegetation play an important role in the chemistry of the atmosphere due to the magnitude of biogenic VOC emissions and their high reactivity with other trace atmospheric constituents. On a global scale, biogenic emissions of VOCs are estimated to exceed anthropogenic emissions by roughly a factor of ten. On a regional scale in and downwind of urban areas the relative importance of anthropogenic and biogenic VOC emissions is dependent on the rates of anthropogenic emissions, the type and density of vegetation and the light and temperature conditions that drive biogenic emissions. Accurate in-situ measurements of biogenic emissions of VOCs are crucial for our understanding of both the environmental parameters controlling emissions and their effects on tropospheric ozone and aerosol formation. Substantial knowledge has accumulated on biogenic isoprene and monoterpene emission rates; however there has been a severe lack of data on emissions of oxygenated VOCs (OVOCs).

The objectives of this study were to determine rates of biogenic VOC and OVOC emissions from one of the dominant conifer ecosystems of California. Specifically, the objectives included developing and deploying a new measurement system for ecosystem scale biogenic emissions of 2-methyl-3-buten-2-ol (MBO), acetone, monoterpenes, and other oxygenated hydrocarbons, and supporting the California Air Resources Board use of this data to validate their biogenic emissions inventory system (BEIGIS).

To measure biogenic VOC emissions, we interfaced our existing fully automated in-situ instrument for VOC and OVOC measurements with a Relaxed Eddy Accumulation (REA) system and deployed it in a ponderosa pine plantation (a key ecosystem for MBO and monoterpene emissions) in the Sierra Nevada Mountains. We collected the first canopy-scale, continuous, long-term flux measurements of a suite of VOCs and OVOCs and the environmental variables that regulate them. The field study data was analyzed to understand the ecological and physical processes that control emission rates for use in improving and developing emission model algorithms.

Major findings of this study include:

1. OVOCs were predominantly of natural origin. However, the relative impact of biogenic and anthropogenic emissions was different for each individual OVOC. MBO emissions were completely of biogenic origin, whereas methanol, ethanol, acetone, and acetaldehyde all had a combination of anthropogenic and biogenic sources.
2. Compounds that were biogenically emitted included MBO, methanol, ethanol, acetaldehyde, acetone, and several monoterpenes. These compounds were also the most abundant VOCs at this site, excluding methane, and biogenic compounds dominated the total VOC reactivity in the region. The OVOCs were highly correlated with each other, especially during daytime.
3. Fluxes were dominated by MBO and methanol with daytime average emissions of ~1.3 mg C m^{-2} h^{-1}. Ethanol, acetaldehyde, monoterpene, and acetone fluxes were approximately a factor of 5 lower. All fluxes showed diurnal cycles with maxima around noon and minima at night.
4. Temperature and light were the main drivers for the MBO emissions, and the canopy level flux responses were virtually identical with previously measured leaf level fluxes from ponderosa pine trees at the same site.
5. Ambient temperature appeared to be the most important driver of the other VOC fluxes, but moisture also played a role, particularly for monoterpenes, ethanol and acetone. Humidity impacts monoterpene fluxes particularly during extreme events, such as summer rain storms or prolonged summer droughts, both relatively common in the Mediterranean climate of the Sierra Nevada mountains.
6. Soil and litter emissions, measured using a Pyrex glass chamber, contributed significantly to the canopy level fluxes of methanol, acetaldehyde, monoterpenes and acetone, and had a much smaller contribution to the canopy fluxes of ethanol.
7. Analyses of concentrations of ozone, isoprene and isoprene's oxidation products showed that a substantial amount of the ozone observed at the mid elevations of the Sierra Nevada Mountains was formed through oxidation of biogenically emitted isoprene. On hot days when isoprene emissions were highest, ozone production in this region was dominated (more than 50%) by isoprene oxidation.

Important implications of this study include:

1. Emissions of OVOCs, largely underrepresented in field and laboratory measurements so far, are a substantial component of total biogenic VOC fluxes. Our measurements, and the analytical tools we have developed, will allow improvement of earlier estimates of their emissions, but more laboratory and field measurements are necessary in other important ecosystems before broad-scale conclusions should be drawn. Also, more investigations into litter and soil emissions are needed to determine which ecosystem components are dominating the OVOC emissions and how they respond to environmental drivers.
2. In view of their potential impact on secondary aerosol formation, it is worthwhile to further study the humidity effect on monoterpene emissions, including different plant species and how ambient humidity levels may change both the amount and composition of emitted monoterpenes. It is also necessary to study emission rates of the less abundant monoterpenes because they can provide an important contribution to the sum of all monoterpenes that form secondary aerosols.
3. Isoprene oxidation is far more important in ozone formation compared to anthropogenic VOCs just 80 kilometers downwind from Sacramento. Isoprene is emitted from oak trees in the Sierra Nevada foothills and transported up the western slope during the daytime in summer, along with anthropogenic nitrogen oxides emitted mostly in the Sacramento region. Due to the large natural emissions of isoprene in the foothills, control strategies to reduce ozone in the Sierra Nevada will need to focus on anthropogenic nitrogen oxide (rather than VOC) emissions in the valley below.

DISCLAIMER

The statements and conclusions in this report are those of the authors from the University of California and not necessarily those of the California Air Resources Board. The mention of commercial products, their source, or their use in connection with material reported herein is not to be construed as actual or implied endorsement of such products.

Whole Ecosystem Measurements of Biogenic Hydrocarbon Emissions

1. Introduction

In many regions across the United States, the production of tropospheric ozone is impacted as much or more by the photochemical reactivity of hydrocarbons emitted from plants as by hydrocarbons emitted from vehicles and industry. The mix of hydrocarbon and nitrogen oxides emissions control strategies in many regions thus relies on proper understanding of the magnitude of biogenic emissions and the chemistry of these biogenic hydrocarbons. In addition, biogenic hydrocarbons react in the atmosphere to form fine aerosols.

1.1. Objectives

The objectives of this study were to utilize the relaxed eddy accumulation technique to determine rates of biogenic oxygenated volatile organic carbon (OVOC) and other volatile organic carbon (VOC) emissions at the ecosystem scale above one of the dominant conifer ecosystems of California.

Specific objectives included:

1. Develop emission factors for methylbutenol, acetone, terpenes, and other oxygenated hydrocarbons.
2. Study ecosystem biogenic emission fluxes and support ARB use of this data to validate BEIGIS.

To accomplish these objectives, technical objectives included:

i) Interface our existing automated in-situ instrument for VOC and OVOC measurements with a Relaxed Eddy Accumulation (REA) system.

ii) Deploy this measurement system in a ponderosa pine plantation (a key ecosystem for methylbutenol and terpene emissions) in the Sierra Nevada Mountains to measure ecosystem scale biogenic emissions.

iii) Create a database of VOC and OVOC emission rates and the environmental variables that regulate them.

iv) Analyze the field study data to further understand the ecological and

physical processes that control biogenic emission rates and to improve and develop emission model algorithms. These algorithms are crucial input for atmospheric chemistry models to investigate the relative impact of biogenic and anthropogenic VOC emissions on tropospheric ozone production.

1.2. Background

Volatile Organic Carbon (VOC) is emitted to the atmosphere in substantial quantities from both anthropogenic and biogenic sources [*Fehsenfeld et al.*, 1992; *Singh and Zimmerman*, 1992]. VOCs play key roles in tropospheric chemistry, but perhaps most importantly, they react with oxides of nitrogen in the presence of sunlight to produce tropospheric ozone [*Trainer et al.*, 1987; *Chameides et al.*, 1988]. Ozone is known to be toxic to plants at concentrations which are often measured in agricultural and forested areas of California [*Heck and Brandt*, 1977; *Peterson et al.*, 1987], and there is currently significant concern over ozone injury to forest ecosystems of the Sierra Nevada [*Ooy et al.*, 1995; *Salardino and Carroll*, 1998].

National programs to reduce tropospheric ozone production have been particularly less successful in areas with substantial biogenic VOC emissions. Strategies for ozone abatement in the United States have focused mainly on reductions of anthropogenic VOC emissions, however urban and rural areas in the United States continue to exceed the national ambient air quality standards for ozone [*Schere*, 1988]. Recent national annual emission estimates by Placet [1990] suggest that approximately 60% of the total hydrocarbons emitted are from biogenic sources, and that in the summer when tropospheric ozone production rates are highest, biogenic emissions account for approximately 77% of the total. Photochemical modeling studies have shown that ozone production in many regions of United States is quite sensitive to biogenic emissions of VOC [*McKeen et al.*, 1991; *Chameides et al.*, 1988] and that uncertainty in emission rates introduces large uncertainty into analyses of the efficacy of regulations to reduce

anthropogenic emissions of VOC or NO_X.

Biogenic VOC emission data are still quite limited compared to the number of plant species which may emit them [*Fehsenfeld et al.*, 1992]. Isoprene and terpenes are assumed to be the dominant VOC compounds emitted from the terrestrial biosphere, representing the largest global input of non-methane hydrocarbons to the atmosphere. Other hydrocarbons make up 30 to 50% of the biogenic total [*Zimmerman*, 1979; *Winer et al.*, 1989; *Singh and Zimmerman*, 1992], and little information is available on the factors which control their emissions.

Effective ozone abatement strategies cannot be developed without quantitative understanding of biogenic VOC emissions rates [*National Research Council*, 1991]. Decision-makers must know whether limiting anthropogenic VOC emissions in industrialized regions can significantly curb photochemical ozone production.

1.3. Previous Work and Outlook at the Beginning of This Study

Vegetation was first recognized as an important source of VOC to the atmosphere by Went [1955]. Isoprene and terpenes were soon identified as being emitted from leaves [*Sanadze*, 1957; *Rasmussen*, 1970], and they are currently believed to be the dominant VOC compounds emitted from the terrestrial biosphere. Most field and laboratory studies have focused on isoprene and terpenes, however it has become evident over the last 30 years that the biosphere emits a wide range of VOC species including a variety of alkanes, alkenes, alcohols, ketones, and aldehydes [*Zimmerman et al*., 1979; *Isodorov et al.*, 1985; *König et al*., 1995, *Goldstein et al*., 1996, *Kesselmeier et al*., 1997; *Janson et al*., 1999]. Emissions of a wide variety of VOCs and OVOCs have been observed from agricultural and natural plants which grow in the Central Valley of California using enclosure measurements performed in the laboratory and under field conditions [*Arey et al.*, 1991; *Winer et al.*, 1989].

2-methyl-3-buten-2-ol (methylbutenol, MBO), first identified in VOC

emissions from ponderosa pine by *Knoeppel et al*. [1980], was recently measured at high concentrations in a forested region of Colorado, with a diurnal cycle similar to isoprene, indicating that its source was biogenic [*Goldan, et al*. 1993]. Subsequently, leaf level emission measurements have shown that MBO is emitted in significant quantities from the needles of several pine species including ponderosa pine and lodgepole pine, and suggest that the emitting species are mostly restricted to western North America [*Harley et al*., 1998]. Basal emission rates reported for MBO from these pine species are similar to basal emission rates of isoprene from oak trees. Ponderosa pine composes over 20% of forest canopy cover in many western states, and lodgepole pine is similarly dominant (Chris Geron, personal communication based on USDA forest statistics). Emissions of MBO from these two species represent a potentially dominant source of biogenic hydrocarbon emissions in California and in the western North America.

We continuously measured concentrations of a wide range of VOC and OVOC compounds at 45 minute intervals above a ponderosa pine plantation in California (Blodgett Forest Research Station, 4000 feet elevation, ~50 miles east of Sacramento, see section 2.3.1) from July 2 – August 5, 1997, and again in July through October 1998. MBO concentrations were consistently higher than isoprene, typically reaching 2 ppb in the afternoon, with occasional peaks up to 4 ppb [*Lamanna and Goldstein*, 1998]. Concentrations of terpenes (sum of α-pinene, 3-carene, d-limonene) never exceeded 0.4 ppb during the daytime. Our measurements suggested that MBO was among the most abundant biogenically emitted hydrocarbons in this region.

Biogenic VOC emission from plants has been measured in natural environments using branch or leaf enclosure [*Zimmerman*, 1979; *Lamb et al*., 1985; *Lamb et al*., 1986; *Khalil and Rasmussen*, 1992; *Fuentes et al*., 1995], tracer release [*Lamb et al*., 1986], and micrometeorological techniques *[Knoerr and Mowry*, 1981; *Lamb et al.*, 1985; *Goldstein et al*., 1995; *Goldstein et al*., 1998], and in controlled laboratory settings [*Sanadze*, 1969; *Tingey et al*., 1979; *Monson and Fall*, 1989; *Guenther et al*., 1991]. Isoprene emission rates in the

field were observed to depend on both light and temperature, and varied from zero at night to up to a few percent of the photosynthetic carbon uptake by the plants during the day. Laboratory and field studies have demonstrated that most monoterpene emissions are affected by leaf temperature but not by light, and that emission rates are strongly associated with terpene vapor pressures [*Tingey et al*., 1980; *Juuti et al.*, 1990; *Guenther et al*., 1991]. MBO emission rates have been shown to depend on both light and temperature, in a similar manner as isoprene [*Harley et al*., 1998]. Considerably less information is available on the factors that control emissions of other VOC compounds.

Continuous measurements of whole ecosystem VOC and OVOC emissions over time scales from hours to seasons are critical for identifying inadequacies in our knowledge of biogenic emissions and improving understanding of the processes which control them. Enclosure measurements are extremely useful for identifying the major compounds emitted from specific plant species, for surveying a wide variety of species, and for determining their response to controlled changes in conditions. However, there are significant disadvantages to enclosure techniques including:

(1) Emissions are not measured in the plant's natural environment, so the response of emission rates to natural variability of the environment is not observed,

(2) plants can easily be injured during enclosure measurements and many VOCs are emitted in response to plant injury, and

(3) it is difficult to accurately estimate ecosystem and regional scale emission rates based on single plant (usually leaf or branch) enclosure measurements.

This project was motivated by the need for new measurements to determine rates of biogenic VOC and OVOC emissions at the ecosystem scale. Data were needed on VOC and OVOC emission rates (particularly MBO, acetone, and monoterpenes) for key ecosystems in the Western United States. There was a

severe lack of whole ecosystem emission measurements in coniferous ecosystems. It is important to measure how emissions change with natural variations of temperature, photosynthetically active radiation (PAR), water availability, and time (season). The most direct and accurate way to determine these factors is with continuous whole ecosystem flux measurements that observe the natural climatic variability and do not disturb the vegetation. This report describes our efforts to address this need for new data and understanding on biogenic VOC and OVOC emissions from a dominant coniferous ecosystem in California.

2. Field Measurement Site

The measurement site near Blodgett Forest Research Station (38°53'42.9"N, 120°37'57.9"W, 1315 m elevation) on the western slope of the Sierra Nevada mountains has been extensively described by *Goldstein et al.* [2000] (Figure 1). The site is characterized by a Mediterranean climate with predominant rainfall between September and May and almost no rain during the summer months. It consists of a typical clear-cut plot (owned by Sierra Pacific Industries, SPI), planted with *Pinus ponderosa* L. in 1990. Large amounts of woody litter and stumps can still be found throughout the plantation. Among the pines there are also a few individuals of douglas fir (*Pseudotsuga menziesii*), white fir (*Abies concolor*), black oak (*Quercus kellogii*), and incense cedar (*Calocedrus decurrens*). The understory was dominated by manzanita (*Arctostaphylos* spp.) and whitethorn (*Ceonothus cordulatus*), which, however, was almost completely cut throughout the plantation in spring 1999. Extensive biomass surveys were done in 1999 and 2000. Ponderosa pine ground coverage, tree height and DBH were measured throughout a 200×10 m transect extending from the measurement tower to the SW, the main daytime wind direction. Leaf area index (LAI) and biomass density for each needle age class was calculated from allometric measurements on 17 cut trees [*Xu*, 2000]. Leaf area during summer 1999 was extrapolated from periodic leaf elongation measurements. It reached a maximum of ~4 (all-sided) at the end of the growing season. Specific leaf weight averaged 100 and 120 g m^{-2} for current-year and older ponderosa pine needles (all-sided).

A walk-up tower was erected in 1997, when the trees were 6-7 years old and 3-4 meters tall. Meteorological data and trace gas mixing ratios and fluxes (CO_2, H_2O, O_3, and hydrocarbons) were measured approximately 5-6 m above the average tree height [*Lamanna and Goldstein*, 1999; *Schade et al.*, 1999; *Baker et al.*, 1999; *Goldstein et al.*, 2000; *Bauer et al.*, 2000; *Goldstein and Schade*, 2000; *Schade et al*., 2000; *Schade and Goldstein*, 2001]. The tower fetch area extends approximately 200 m to the SW during daytime. The nighttime fetch is less well defined but generally lies in the opposite, NE direction. For the REA system, a three-dimensional sonic anemometer (Campbell Scientific), run by a CR23X data logger, was mounted approximately 11 m above ground on a ~2 m beam extending to the SW.

3. Experimental Methods

3.1 Hydrocarbon Measurements

The majority of VOC field measurements have focused on an apparently incomplete subset of compounds. This limited focus results mainly from a historic inability to accurately collect and analyze OVOCs. For this study we used an instrument designed and built in our laboratory for automated in situ measurements of a wider range of VOCs. Capillary gas chromatography is the most common method for analyzing VOCs in ambient air samples. A typical gas chromatography (GC) system consists of components that provide for sample collection, enrichment, separation, identification, and quantification. The suite of target compounds to be measured determines system component selection for instrumentation development. We designed and built an instrument to specifically focus on measuring MBO, isoprene and its oxidation products methyl vinyl ketone (MVK) and methacrolein (MACR), acetone, acetaldehyde, and terpenes, in situ (as described in *Lamanna and Goldstein* [1999], *Schade et al.* [1999], and *Schade and Goldstein* [2001]). In addition, our instrument operates without the use of liquid nitrogen, thus extending the timeframe and physical range of sites where continuous measurements can be obtained. This instrument has two independent measurement channels and was designed to be easily adapted to any of three continuous in situ sampling schemes: relaxed eddy accumulation (REA) flux, gradient flux, or ambient concentration measurements. For this study, the system was configured to measure fluxes by REA.

The main sample intake was mounted on a walk-up tower (Upright Towers, Selma, California) ~6 m above the forest canopy (11 m above ground level). Ambient air was drawn at 10 L min^{-1} STP through 2 μm Teflon particulate filters (Gelman Sciences, Ann Arbor, Michigan) and 16 m of 3/8 inch OD, 1/4 inch ID Teflon tubing (Chemfluor-Norton Performance Plastics, Wayne, New Jersey) into the instrument shed at ground level, where the flow rate was controlled (MKS Instruments, Andover, Massachusetts). Two separate subsamples from the airstream were drawn from the center of the main sample tube at 15 cm^3 min^{-1} STP through 0.030 inch ID fused silica lined stainless steel

tubing (Silcosteel, Restek, Bellefonte, Pennsylvania). With the valve array in sampling mode, the subsamples flowed through a pretreatment trap to remove ozone (KI-impregnated glass wool, following *Greenberg et al*. [1994]), and then into the sample traps mounted in the cold block (-10°C) where the target analytes were concentrated onto a pair of Silcosteel© microtraps, sequentially filled with a small amount of glass beads, and approximately equal amounts of Carbopack B and Carbosieve SIII (~12 mg, Supelco Inc). The cold block imbedding the microtraps was cooled with two 7.5 A thermoelectric elements (Ferrotec America Corporation, Manchester, New Hampshire). Laboratory tests showed that no breakthrough of the compounds of interest occurred at trap temperatures below -2°C for a sample size of 210 mL. This was done by analyzing dynamic dilutions of ppm standards (see below) into ambient air up to mixing ratios of approximately twice as high as expected at the field site. In the field the cold block temperature was kept between -5° and -10°C during sampling, and the sample size was never larger than 150 mL. After collection the samples were thermally desorbed on-column (250°C for 1.2 min), separated by two 60 m, 1 μm film Rtx-WAX columns with 5 m retention gaps, and detected by two FIDs (a sample chromatogram is given in Figure 2). The setup was fully automated (HP Chemstation and Campbell Scientific data logger) and measured a pair of 30 min average samples in situ once every hour.

The system was calibrated by automatic dilution of primary ppm level gas standards (Scott Marrin Inc., Riverside, CA) into the tower sampling line every 10 hours to achieve low-ppb and sub-ppb standard additions. The National Center for Atmospheric Research (NCAR) OVOC I standard [*Apel et al.*, 1998] was used to calibrate acetaldehyde and ethanol. Both calibrations were ~30% higher than their molecules theoretical FID responses referenced to isoprene, assuming that the given mixing ratios were correct. Values reported throughout this report have been calculated using the theoretical FID response factors instead [*Lamanna and Goldstein*, 1999]. Acetone and MBO were calibrated with two Scott-Marrin standards, and their response factors matched the theoretical FID response as referenced to isoprene. Calibration amounts were typically varied over 1-2 week periods between ~0.5 and ~10 ppb. Correlations with r^2 values of better than 0.95 were achieved, and no systematic change in instrument

response was observed over time.

Methanol coeluted with MEK and 3-methyl furan and was not successfully calibrated on the WAX columns because the methanol standard also contained MEK. However, methanol separation was achieved for a few samples in June 1999 on a DB-624 column, and the FID response factor (using NCAR OVOC I [*Apel et al*., 1998]) was consistent with its theoretical response factor, which was thus used for calibration.

OVOC mixing ratios were more precisely determined in 1999 compared to previous measurements with this instrument in 1998 [*Schade et al*., 2000]. Rapidly switching between sample and zero air in the REA setup improved the chromatography because water, which interferes with the sampling, desorption, and chromatographic processes, was constantly purged from the traps. However, using this setup, methanol coeluted with MEK and 3-methyl furan. We corrected both updraft and downdraft measurements for these biases assuming that the MEK abundance was ~1/14 of that of acetone, based on tight correlations between these compounds in July 1997 and June 1999 at the same site (data not shown), and that the 3-methyl furan abundance was 1/25 of that of isoprene, based on its yield from isoprene photooxidation [*Ruppert and Becker*, 2000] and assuming that its loss rate is similar to that of isoprene. No correction was made for the other OVOCs.

In order to estimate the OVOC flux contribution from the soil compartments of the ecosystem we carried out a limited set of enclosure measurements. A Pyrex glass chamber covered with light-transparent Teflon foil [*Schade et al*., 1999a] was placed on the ground near the measurement tower. A spot that was in full sunlight throughout most of the day was chosen in order to monitor a larger range of different temperatures inside the chamber. That temperature was measured with a thermocouple placed inside the litter layer or in the topsoil (upper 1 cm), avoiding radiation loading.

The chamber was flushed with the same zero air used for the FIDs and to run instrument blanks. Flow to the chamber was mechanically regulated to approximately 8 L min^{-1} under ambient conditions, and chamber air was extracted at 1-2 L min^{-1} by moving the sampling line from the measurement tower to the soil chamber. Excess air escaped the chamber mostly through small holes in the cover foil [*Schade et al*., 1999a], and the

chamber was set for much higher inflow than sample flow to avoid turbulent mixing of air from outside with chamber air. Subsamples of 150 mL were preconcentrated over 30 min periods from the main sample stream onto the hydrocarbon microtraps and analyzed in the same manner as described above. OVOC fluxes were calculated from the difference in mixing ratio between chamber blanks and original samples, multiplied by the flow through the chamber, and referenced to the chamber ground area. Chamber blanks were measured by covering the ground with another sheet of Teflon foil during sampling. Only small differences could be found between these chamber blanks and direct measurements of the zero air, except for methanol, for which a larger carry-over effect occurred after very high mixing ratios in the chamber.

3.2 REA System

Ecosystem scale flux measurements of some scalars can be measured by eddy correlation (EC). In an EC measurement, the flux is calculated from the covariance of the vertical wind velocity with the scalar of interest (e.g. CO_2, H_2O, air temperature etc.). In order to use the EC method, measurements of scalars must be accomplished with time resolution fast enough to resolve changes associated with turbulent eddies (referred to as “updrafts” and “downdrafts” in the vertical wind), e.g. faster than 1 second above a forest. When this project was started, such instruments were unavailable for the particular suite of VOC compounds of interest. Thus, we needed a different experimental approach with less stringent sample analysis requirements. We chose an approach that interfaces our automated in-situ instrument described above with a Relaxed Eddy Accumulation (REA) system for ecosystem scale flux measurements. The REA technique is now seen as a stable flux technique comparable to well accepted eddy correlation systems [e.g. *Delon, et al*., 2000]. This system allows simultaneous flux measurements for all the VOC and OVOC compounds separated in our analytical system. Our experimental approach is powerful because it allows for simultaneous measurement of the magnitude of each individual compound, and the range of compounds, being exchanged between the ecosystem and the atmosphere.

The relaxed eddy accumulator "accumulates" air that is entering or leaving

the ecosystem by sampling updrafts and downdrafts separately. Flux densities are estimated using the equation [*Businger and Oncley*, 1990; *Nie et al*., 1995; 1996]:

$$F = b\ \sigma_w (C_u - C_d) \qquad (1)$$

F is the flux, b is an empirical coefficient, $C_u - C_d$ is the mean difference in concentration between the updrafts and downdrafts, and σ_w is the standard deviation of the vertical wind speed. The experimental setup utilizes a fast solenoid valve (~10 Hz) that switches the sampling path based on changes in the vertical wind direction as measured by a sonic anemometer. Updrafts and downdrafts are collected separately and analyzed for speciated VOCs and OVOCs using the dual channel gas chromatograph described above.

A schematic representation of the REA system interfaced with the GC is shown in Figure 3. Similar to the method of *Nie et al.* [1995], a single sampling line (~16 m 3/8" ID Teflon PFA) ran from next to the sonic anemometer to the sampling system inside the temperature-controlled instrument building. Laboratory tests showed that even a high flow of ~30 L min^{-1} taken from beside the anemometer did not influence the wind measurements noticeably. In the field a constant flow of 10 L min^{-1} was set using a flow controller. The residence time in the tubing was 2.3 ± 0.2 s (3 standard deviations, $N = 7$), determined by popping balloons near the anemometer and measuring the lag time between the sonic spike and the onset of the CO_2 response in an infrared analyzer (LICOR 6262). For the REA measurements, updrafts and downdrafts were subsampled from within the main sample stream and separated with Teflon segregator valves (General Valve/Parker, Fairfield, New Jersey) when the vertical wind speed *w* exceeded a deadband of 0.6 × σ_w [*Oncley et al*., 1993], using a 5 min running average of w and its standard deviation σ_w [*Guenther et al*., 1996]. Because of a slightly shorter gas path in the final setup a delay of 2.2 s was input to the data logger that switched the segregator valves. The valves switched between sampling zero air (from a zero air generator, AADCO, Clearwater, Florida) and sampling ambient air by closing a normally open valve and opening a normally closed valve simultaneously. The zero air was sampled in bypass and was adjusted to the tower sampling line pressure (P_1 versus P_2) as shown in

Figure 3, using several meters of 1/8" tubing to provide further resistance to a needle-valve-controlled vacuum. Samples were collected onto the microtraps at a flow rate of 15 mL min^{-1} maintained by one flow controller per line. Sample size was determined by summing the times when a segregator valve was "open" during the half-hour period and was typically on the order of 120 mL (STP) during the day. The standard deviation of the measured flow served as an indicator of potentially unstable sampling due to sudden pressure changes, which could have occurred if sample and zero air pressure were different. Data collected during times when this standard deviation exceeded 0.2 ml min^{-1} (>1%) were discarded.

Systematic differences between the measurement channels can lead to data misinterpretations. We chose the isoprene oxidation product methacrolein (MACR) as a reference for a channel intercomparison on a measurement basis. We could detect neither emission nor deposition of MACR in our ecosystem; it elutes from the WAX column without interference and is generally present at mixing ratios above 0.2 ppb in summer. Measurements in 1998 showed no systematic differences between the channels with a r^2 of 0.96. During extended parts of the measurement period in summer 1999, systematic differences between the MACR peaks occurred that were later identified as an improperly shutting valve on one of the segregator valve setups. Data were corrected for this dilution with zero air by using MACR as a reference peak, that is, by multiplying the measured mixing ratios of the diluted channel by the ratio of the MACR mixing ratios between the two channels for each sample. The adjustment was applied to the complete data set and ranged from 0.6 up to a factor of 4 with a 0.1-0.9 quantile range of 0.8-1.8.

The major advantages of this analytical system include its full automation, enabling unattended sampling over several day periods (not possible with existing cartridge REA systems), its having no electronic or valve equipment exposed to the elements, and its one-dimensional automated in situ chromatography for the OVOCs. The lag time was extremely stable because we controlled the flow through the main sampling line. Because of the potential "smearing" of smaller eddies inside a long sampling line like ours [*Lenschow and Raupach*, 1991], a deadband was used to reduce sampling of small eddies.

3.3 Additional Measurements at Blodgett Forest

The Blodgett Forest measurement site is officially part of the AmeriFlux and FluxNet networks with Allen Goldstein as Principal Investigator. These networks are an international scientific effort aimed at guiding, collecting, synthesizing, and disseminating long-term measurements of CO_2, water, and energy exchange from a variety of ecosystems. As part of this effort, fluxes of CO_2, H_2O, and sensible heat are continuously measured by the eddy covariance method at Blodgett Forest [e.g. *Goldstein et al*., 2000]. Environmental parameters such as wind direction and speed, air temperature and humidity, net and photosynthetically active radiation (R_n and PAR, respectively), soil temperature, soil moisture, soil heat flux, rain, and atmospheric pressure are also monitored. Additional continuous measurements at the site included O_3 concentration and flux [*Bauer et al*., 2000]. The data acquisition system is separated in two parts: (1) a fast response system which monitors data at high frequency (up to 10 Hz) used to calculate eddy covariance, with raw data stored in 30-minute data sets; and (2) a slow response system which monitors environmental parameters stored as 30-minute averaged data.

Wind velocity and virtual temperature fluctuations were measured at 10 Hz with a three-dimensional sonic anemometer (ATI Electronics Inc., Boulder, CO) mounted on a horizontal beam at 11 m above the ground (~ 6 m above the trees), 3 m upwind (daytime) of the tower. CO_2 and H_2O mixing ratios were measured with an infrared gas analyzer (IRGA, LICOR model 6262, Lincoln, NE). See *Goldstein et al*. [2000] for a complete description of these measurements.

Environmental parameters were recorded on a CR10X data logger (Campbell Scientific Inc., Logan, UT). The wind monitor (R.M. Young, Traverse City MI), relative humidity (Vaisala Inc., Woburn MA) and temperature probe (Fenwal Electronics Inc.), net radiation (REBS, Seattle WA) and PAR (Li-Cor Inc., Lincoln NE) sensors were located on a beam at the top of the tower, and vertical profiles were measured at four heights for temperature and relative humidity, and three heights for wind speed using spinning cup anemometers (Met-One Inc., Grants Pass, OR). Ten soil temperature thermistors (Campbell Scientific Inc.) were placed at depths ranging from 5 to 50 cm below the soil surface, spread in three vertical locations. Three heat flux plates (REBS,

Seattle WA) were placed at 10 cm depth next to a soil thermistor. Two soil moisture probes (Campbell Scientific Inc., Logan UT) were buried horizontally at 10 and 20 cm depth. Vertical profile measurements of CO_2 and H_2O were made using a Li-Cor 6262 IRGA (Li-Cor Inc., Lincoln NE) which sampled at five heights sequentially for six minutes each. In 1999, leaf temperatures and leaf wetness (Campbell Scientific, Logan, Utah) were measured at four locations on a single tree near the tower.

Seasonal meteorological data including the period for which VOC measurements are reported are given in Figure 4. They illustrate the last major rain event in the spring (beginning of June) and first major event in the fall (end of October), the seasonal decrease in soil moisture leading to drought-stress, as well as summer air temperatures and humidities representative for the Mediterranean climate at these elevations.

4. Results and Discussion

4.1 Mixing Ratios

Mixing ratios were measured for the compounds listed in Table 1. The daytime and nighttime mean concentrations are listed for each compound. An electronic copy of the full data set has been submitted with this report, and is described in appendix A.

Table 1. Average Daytime (1000–1730 PST), and Nighttime (2200–0530 PST) (O)VOC Concentrations and Fluxes From the Canopy-Scale Measurements.

	Mixing ratios[a]		Fluxes[b]	
	Daytime	Nighttime	Daytime	Nighttime
MTBE	0.04	0.04	NA[c]	NA
Toluene	0.08	0.06	NA	NA
MBO	1.78	0.50	1.37	0.01
Isoprene	0.69	0.39	<0.01	<0.01
MVK	0.76	0.71[d]	-0.01	-0.01
MACR	0.49	0.43	NA[d]	NA[d]
β-pinene	0.09	0.17	0.20[d]	0.05[d]
α-pinene	0.07	0.16	0.10	0.01
Δ-3-carene	0.08	0.09	0.13[d]	<0.01[d]
Acetaldehyde	1.41	2.16	0.14	0.02
Acetone	2.69	3.11	0.21	0.02
Methanol	10.51	12.7	1.09	0.25
Ethanol	1.18	2.69	0.27	0.10

[a] Concentrations are in ppb (mean of 0.1-0.9 quantile, rounded).
[b] Fluxes are in mg C m^{-2} h^{-1}
[c] NA: not applicable (= flux not detectable).
[d] see data set documentation for further comments

4.1.1 Isoprene and Its Atmospheric Reaction Products

Isoprene and its atmospheric reaction products methacrolein (MACR) and methyl-vinyl-ketone (MVK) [*Montzka et al*., 1993] were almost always above the detection limit throughout the 1999 measurement period, and we include for comparison some discussion of measurements done in both 1997 and 1998. Another, minor reaction product, 3-methyl-furan, coelutes with methanol and could therefore not be quantified. MACR was calibrated with two different standards, and its response factor referenced to

isoprene. MVK was not calibrated directly but its response factor on the FID was assumed to equal that of MACR due to the similar molecular structure and same carbon content.

Summer (July/August) mixing ratios of isoprene, MACR and MVK were 0.05-1.38 ppb (0.2-1.7 ppb; 0.22-1.52 ppb), 0.1-1.0 ppb (0.1-0.8 ppb; 0.3-1.05 ppb), and 0.24-1.72 ppb (0.1-1.4 ppb; 0.35-1.72 ppb) in the years 1999, 1998, and 1997 respectively, and are given here as their 0.1-0.9 quantile ranges. No significant direct fluxes of these three compounds were detected from the plantation itself. Mixing ratios of MACR and MVK were always highly correlated ($r^2 \geq 0.8$), whereas their correlation with their atmospheric precursor isoprene was generally weaker. An explanation for this can be found in the diurnal cycles of isoprene and its oxidation products shown in Figure 5. Mixing ratios of all three compounds regularly increase before noontime (Pacific Standard Time, PST), 2-3 hours after the wind shifts directions and begins coming from the southwest. The air transported up the western slope of the Sierra Nevada during the day picks up isoprene emissions mostly at elevations below 1000 m in the "foothills" of the Sierra. Oak woodlands, consisting of Interior Live Oak (*Quercus wislizeni*), Canyon Live Oak (*Quercus chrysolepsis*), Black oak (*Quercus kelloggii*), and Blue Oak (*Quercus douglasii*), can be found 30-40 kilometers upwind of the measurement site (Figure 1). Wind speeds of 3-4 m s^{-1} during the morning are consistent with a 2-3 hour transport time from this large area source of isoprene. Further up the Sierra Nevada, isoprene sources rapidly diminish as conifers replace oaks. Nevertheless, a smaller isoprene source is expected to exist throughout the lower elevations west of our measurement site. At elevations above 1000 m, Black Oak is the dominant isoprene emitter. The density of Black Oak around our measurement site is very low because the land use concentrates on timber production. However, Blodgett Forest land directly to the west of the measurement site has a higher density of Black Oak, and isoprene emissions probably from these trees can be detected in the diurnal isoprene cycles during hot days, as can be noted around 8 am in Figure 5. On these hot days, the isoprene mixing ratio increases simultaneously with that of methylbutenol in the early morning because emissions of both compounds are driven by sunlight. During this morning increase, the correlation

between isoprene and its oxidation products is poor, because there is not enough time to oxidize locally emitted isoprene before the air mass travels past the measurement site. Around noontime isoprene mixing ratios increase again along with its oxidation products, as air is transported to the site presumably after a larger input of isoprene 30-40 km up-wind.

The diurnal cycle of isoprene and its oxidation products is very reproducible for days with the typical diurnal up-slope/down-slope transport pattern experienced during the summer. During the up-slope transport of isoprene, MACR and MVK are produced and consumed by photochemistry dominated by the OH radical. The relative production rate of MVK to MACR under high NO_x conditions is approximately 1.4 [*Paulson et al*., 1992], the relative destruction rate (reaction with the OH radical) approximately 0.56. Under intense photochemistry with constant isoprene input this would lead to a steady state MVK to MACR ratio of ~2.4 in the afternoon. At our measurement site, the MVK to MACR ratio rapidly increases in the photochemically aged air mass transported from the lower elevations, and afternoon ratios of 1.4-2.8 (0.1-0.9 quantile; 1998 and 1999 data) are measured. A mean diurnal cycle of this ratio is shown in Figure 6. While the diurnal cycle and the afternoon MVK to MACR ratio is consistent with known isoprene photochemistry, its variability reflects the degree of photochemical processing and the spatial inhomogeneity of isoprene emissions. Higher than steady state MVK to MACR ratios indicate rapidly decreasing isoprene emissions during transport (ratio dominated by loss rates), whereas lower than steady state MVK to MACR ratios indicate the influence of recent isoprene emissions or slow photochemistry (ratio dominated by production rates).

Another ratio that is indicative of the extent of photochemical processing of isoprene emissions, is the MACR+MVK to isoprene ratio. In areas close to emission sources, this has been found to be small [e.g. *Montzka et al*., 1993; 1995]. At the Blodgett Forest site, this ratio is routinely larger than 1, except during those morning hours when local isoprene emissions affect the isoprene mixing ratio significantly. At night when isoprene emissions cease, the ratio often exceeds 2, because chemical removal of isoprene due to ozone (or OH) reactions keep producing MVK and MACR, while the

reactions of MVK and MACR themselves are slower. The high MVK+MACR to isoprene ratio at this site again demonstrates the limited impact of local isoprene emissions compared to those up-wind of the site. The ratio further increases seasonally into the fall when local isoprene emissions stop and isoprene emissions in the foothills decrease (see Figure 7). Figure 7 also includes seasonally smoothed air temperature: As isoprene emissions increase exponentially with temperature, the MVK+MACR to isoprene ratio tends to decrease exponentially with temperature. Air masses arriving at our measurement site then contain little isoprene that is left over after photochemical oxidation during transport in the fall.

4.1.1.1 Ozone Production from Isoprene Oxidation

During its transport upslope from the foothills, isoprene is oxidized producing not only MACR and MVK, but also ozone. During isoprene oxidation two peroxy-radicals are formed that will react with NO to form NO_2 which is subsequently photolyzed to form ozone if more than ~50 ppt NO is present. Due to its proximity to the Central Valley of California with its numerous sources of NO (mainly mobile sources), air in the Sierra Nevada foothills leading up to our measurement site typically has ambient NO mixing ratios above 50 ppt (confirmed by measurements at our site, M. Dillon and R. Cohen, UC Berkeley Chemistry Department, personal communication).

The amount of MVK produced versus ozone produced can be estimated from known isoprene chemistry [*Biesenthal et al.*, 1997]; for every 1 ppb increase of MVK approximately 5 ppb ozone increase can be expected. As photochemistry during transport is fast and will remove some MVK before it reaches our measurement site, there will be some additional ozone production from MVK oxidation during transport, which leads us to an estimated production of ~7 molecules of ozone per molecule of MVK observed at Blodgett Forest. This theoretical estimate can be compared with the simultaneous increase of MVK and ozone we actually observed. For this analysis, we focused on the time window 2-3 hours after the morning wind shift until MVK levels off in the afternoon, when either a steady state MVK mixing ratio is reached or the assumption of all peroxy-radicals reacting with NO no longer holds due to growing competition from

peroxy self reactions. We further limit the analysis to southwest wind directions and minimum detectable changes in both the MVK (+0.1 ppb) and ozone (+2 ppb) mixing ratios. Figure 8 shows all MVK versus all ozone mixing ratios for the time window in question, demonstrating the approach. Comparing the slope of this graph (10-20) to the theoretical slope if all ozone produced were from isoprene oxidation (~7) leads to the conclusion that, on average, 35-70 % of the ozone increase observed at these elevations during summer can be attributed to isoprene oxidation with the help of anthropogenically emitted nitrogen oxide.

We are currently preparing a more detailed, day by day analysis of this relationship (Dreyfus et al., in preparation) in order to reveal the dominant drivers for isoprene's contribution to ozone formation in the Sierra Nevada mountains. Figure 9 shows how the daily slope of MVK versus ozone changes with the sum of isoprene's oxidation products, a proxy for the amount of isoprene oxidized. The slope converges exponentially towards the theoretical slope of ~7 the more isoprene is input to the photochemical system. The exponential influence of air temperature on isoprene emission was identified as a main driver of this relationship. However, a number of outliers suggest there are other significant drivers, such as NO_x availability. With a more complete data set on NO, NO_2, NO_y, and CO, we hope to further refine this analysis using data collected during the 2000 measurement campaign.

4.1.2 2-Methyl-3-buten-2ol (MBO) and Other Oxygenated VOCs

Mixing ratios ranged from 1.1 to 41 ppb for methanol, from 0.1 to 9.6 ppb for ethanol, from 0.1 to 5.8 ppb for acetaldehyde, from 0.3 to 11 ppb for acetone, and from 0 to 7.0 ppb for MBO (all updraft data) (Figure 10). Measured ambient OVOC mixing ratios were in accordance with earlier observations at this and other rural sites for methanol, acetone, acetaldehyde, and MBO [*Goldan et al.*, 1995; *Slemr et al.*, 1996; *Solberg et al.*, 1996; *Frost et al.*, 1998; *Riemer et al.*, 1998; *Apel et al.*, 1998; *Lamanna and Goldstein*, 1999; *Schade et al*., 2000] but were higher for ethanol. Mean diurnal mixing ratio cycles for the OVOCs during a two-week period in July 1999 are shown in Figure 11. Increases in mixing ratio during times of limited vertical mixing are indicative

of local sources and are clearly visible in the evening hours. While MBO showed a typical diurnal cycle with larger mixing ratios during the day and decreasing mixing ratios at night, methanol and acetone were more variable with no distinct diurnal pattern. Acetaldehyde and ethanol showed weak diurnal cycles with generally higher mixing ratios at night, when vertical mixing rates were reduced. In addition, we observed higher ethanol than acetaldehyde mixing ratios at night and the opposite during the day.

Particularly during the daylight hours, but also at night, all OVOC mixing ratios were highly correlated with each other, as shown in Figure 12 for selected compounds. This suggests a common transport or direct emission source and/or common drivers to these OVOC emissions, such as temperature. We estimated biogenic and anthropogenic contributions to the methanol, ethanol, acetaldehyde, and acetone mixing ratios using correlations to compounds of known origin, as described by *Goldstein and Schade* [2000]. OVOC mixing ratios under sunny conditions (PAR > 1300 μmol m^{-2} s^{-1}) were correlated with tracers of both anthropogenic and biogenic sources. We used methyl tertiary butyl ether (MTBE) as a tracer of anthropogenic [*Squillance et al*., 1997; *Stationary Source Division*, 1997], and MBO as a tracer of biogenic sources [*Harley et al.*, 1998]. The overall determination coefficient from a multilinear regression and estimates of the biogenic and anthropogenic contributions to the individual OVOC mixing ratio are shown in Table 2. Calculated "backgrounds" are based on the intercepts plus the slopes times the local background of MTBE, estimated from the MTBE measurements to be at the detection limit of ~0.005 ppb. Average biogenic and anthropogenic contributions to the total mixing ratio were calculated from the slopes times the median MBO or MTBE mixing ratios, divided by the sum including background. No anthropogenic contribution was assumed for ethanol because of a slope with MTBE that was insignificantly different from 0. Note that our estimate of the "anthropogenic" contribution does not discriminate between primary emission and secondary production. It has to be viewed as an upper limit because the local transport scheme with up-slope winds during the day not only advects anthropogenic hydrocarbons to the site, such as MTBE, but also biogenic hydrocarbons, such as isoprene, at the same time. That, for example, results in a correlation between MTBE and isoprene oxidation

products, which most probably do not come from the same source. Therefore we cannot exclude the possibility that some amount of the OVOC correlation with MTBE presented here is simply a result of coadvection. Note also that the values in Table 2 are average values for the whole data set and that they can change with weather conditions and time of day, as discussed below.

Table 2. Biogenic and anthropogenic contributions to ambient OVOC mixing ratios based on results of a Multilinear Regression Analysis[a]

	Intercept Ppb	Slope MTBE	Slope MBO	r^2	"Background" ppb	Contribution[b]	
						Percent Biogenic	Percent Anthropogenic
Methanol	2.70	34.1	3.42	0.39	2.87	34.8	20.0
Ethanol	0.19	-0.48	0.51	0.29	0.18	85.6	NA
Acetaldehyde	0.28	6.65	0.41	0.80	0.31	37.7	34.5
Acetone	0.35	17.41	1.17	0.81	0.43	45.7	38.1

[a] The r^2 denotes the overall determination coefficient, NA, not applicable.
[b] Above background.

We can group the OVOCs measured in this work roughly into three classes according to their atmospheric lifetimes (Table 3): MBO as shorter-lived, acetaldehyde and ethanol as medium-lived, and methanol and acetone as longer-lived trace gases. However, despite these lifetime differences the OVOCs showed remarkably strong daytime intercorrelations.

Table 3. OVOC Lifetimes in Hours[a]

OVOC	OH	Photolysis
MBO	2.1	-
Acetaldehyde	8.8	~92[b]
Ethanol	84	-
Methanol	288	-
Acetone	1272	~2500[c]

[a] A 12 hour daytime average OH abundance of 2×10^6 molecules cm^{-3} was assumed [*Atkinson*, 2000].
[b] From Warneck [2000].
[c] From Gierczak et al. [1998].

Mixing ratios of longer-lived trace gases, such as methanol and acetone, did not

have strong diurnal cycles, such as that of MBO. Changes in the overall abundance of methanol and acetone occurred on longer time scales, associated with changes in regional weather conditions. For example, a dramatic decrease in mixing ratios at the beginning of August (Figure 10) was coincident with unusually cold weather. During August 7-18, daytime temperatures stayed below 20°C, and minimum acetone mixing ratios dropped well below 1 ppb, which we had defined earlier as the regional background under summer conditions [*Goldstein and Schade*, 2000]. A similar change was encountered for all OVOCs in August 1999 and again in late September 1999. This strongly suggests a dominance of biogenic over anthropogenic sources, as the anthropogenic sources are less dependent on temperature. The background values given in Table 2 represent mixing ratios measured during the cold weather regimes encountered. Compared to our earlier analysis for acetone [*Goldstein and Schade*, 2000], these background levels are significantly lower, leading to a higher estimate for the average anthropogenic contribution compared to more typical summer weather conditions. We repeated the OVOC budget analysis for different temperature regimes. The biogenic contribution increased with temperature and above 25°C was roughly 50% higher for both acetone and methanol compared to the average values given in Table 2.

The medium lifetime OVOCs acetaldehyde and ethanol showed small diurnal cycles similar to those of the monoterpenes [*Schade et al.*, 1999b]. Mixing ratios were slightly lower during the day than at night. A main difference between acetaldehyde and ethanol mixing ratios is their contribution of sources: While acetaldehyde sources were explained as partially biogenic and partially anthropogenic by the tracer approach (Table 2), ethanol mixing ratios appeared to be of almost completely biogenic origin. The biogenic contributions to the acetaldehyde mixing ratios were only enhanced by 25% during hot days, compared to 50% for acetone and methanol. The respective anthropogenic contribution changed only slightly, possibly because of enhanced secondary photochemical production from anthropogenic hydrocarbons at higher temperatures.

Ethanol was the only compound without a significant correlation with MTBE, which might be due to the fact that ethanol is used as an alternative fuel oxygenate, and

generally not used in combination with MTBE in California. We presume the ethanol sources to be almost completely biogenic. As ethanol was not emitted in significant amounts from either the soil or the litter, the ponderosa pine trees were likely the dominant regional source. The higher mixing ratios of ethanol at night were probably driven by substantial emissions into a shallower nighttime boundary layer, and concentrations decreased as vertical mixing increased in the morning.

4.1.3 Monoterpenes

Monoterpenes that are routinely measured with the described setup include α-pinene, β-pinene, and Δ-3-carene. Monoterpenes with lower ambient mixing ratios than these are currently detectable but are poorly quantified because of the small sample size (<150 mL). The quantifiable monoterpenes are also the main monoterpenes emitted by *pinus ponderosa* L. [*Lerdau et al*., 1994]. β-pinene tends to be more abundant than α-pinene and Δ-3-carene, consistent with the emission rates from the ponderosa pine trees [*Schade et al*., 1999b]. Mixing ratios (0.1-0.9 quantiles) of α-pinene, β-pinene, and Δ-3-carene varied from 30-280 ppt, 30-320 ppt, and 10-160 ppt in summer 1999, respectively. All monoterpenes were highly correlated with each other in all years [e.g. *Schade et al*., 1999b]. Mixing ratios are typically higher at night (Table 1), when the monoterpene lifetimes are longer and emissions from the ponderosa pines continue into a shallower boundary layer. A typical diurnal cycle is shown in Figure 13.

Rain events can trigger large increases in ambient mixing ratios of monoterpenes due to higher than expected fluxes into shallower boundary layers (shown in detail in [*Schade et al.*, 1999b]). No major rain events occurred in summer 1999, however, a small rain event in August [*Schade and Goldstein*, 2001] was followed by elevated α-pinene mixing ratios (Figure 14) when ambient relative humidity levels exceeded 80%. Such events need to be understood in order to judge their impact on local secondary aerosol formation. The potential for such aerosol formation is higher after rain events when NO_x mixing ratios are lower and monoterpene mixing ratios are higher [*Zhang et al*., 1992].

4.2 Canopy-scale Fluxes

Fluxes were evaluated for the compounds listed in Table 1. The daytime and nighttime mean fluxes are listed for each compound, and compounds without a detectable flux are indicated. An electronic copy of the full data set has been submitted with this report, and is described in appendix A.

Individual compound fluxes, *F*, were calculated from Eq. 1 ($F = b\ \sigma_w (C_u - C_d)$), where *b* was determined from measurements of sensible heat flux and air temperature [*Bowling et al.*, 1998], σ_w is the standard deviation of the vertical wind speed, and C_u and C_d are the mixing ratios in the updrafts and downdrafts, respectively. As shown in Figure 15, this method has a higher uncertainty for small fluxes of sensible heat, usually occurring during times of reduced turbulence at night and the transition periods when the sensible heat flux changes sign in the morning and evening. As *b* was remarkably stable when sensible heat flux was not small, we replaced the calculated value by its mean (0.41) for sensible heat fluxes within ±30 W m^{-2} of zero. In addition, values outside a ±0.2 interval of the mean *b* were discarded. We also filled in a small amount of missing daytime sonic data (2% of the data) with the mean *b*-factor and values for σ_w measured on another sonic anemometer, used to determine the CO_2, water, and ozone fluxes. Fluxes of sensible heat and momentum from the two anemometers showed very good agreement (for sensible heat, slope equals 1.05 and r^2 equals 0.99; for momentum, slope equals 0.87 and r^2 equals 0.98).

Possible systematic errors in *b* were investigated in two ways. First, its dependence on the chosen lag time between the sample entering the line and it being segregated was analyzed using air temperature as measured by the sonic anemometer. A subset is shown in Figure 16. During the daylight hours with high turbulence, *b* was indeed optimized by our chosen lag-time. However, even if the chosen lag-time had been off by as much as 0.5 s, the maximum daytime systematic error would generally have been less then 20%. The potential error grows larger during the transition periods (0715 PST). Under low turbulence conditions at night, *b* generally does not show a distinct minimum at the lag time. However, as shown in Figure 15, air temperature from the sonic anemometer is not a good predictor in this case, because many nighttime sensible heat

fluxes are too low. Under these conditions, sampling occurs more erratically with fewer and shorter eddies being large enough to exceed 0.6 σ_w. - Second, the calculated *b*-factors were plotted versus the atmospheric stability parameter *z/L* (*z* is the measurements height, *L* is the Monin-Obukov length). No dependence on *z/L* was obvious except maybe for the transition periods ($z/L \rightarrow 0$), when the calculated *b*-factors should be viewed with caution because of small sensible heat fluxes.

4.2.1 2-Methyl-3- buten-2-ol (MBO) and Other Oxygenated VOCs

4.2.1.1 MBO

Fluxes were highest for MBO and methanol and showed diurnal cycles for all compounds, depicted in Figures 17a and 17b. Shown are means (median for the methanol data) for each hour over the whole measurement period, whereby the number of available samples per hour ranged from 38 (1415 PST) to 51 (1915 PST). Average daytime fluxes are summarized in Table 1. Based on the minimum detectable difference (95% confidence level) between updrafts and downdrafts, calculated for each OVOC from channel intercomparisons, only methanol and ethanol fluxes were statistically different from zero at night (2200-0500 PST; $p = 0$ for methanol and ethanol). However, nighttime mean fluxes of acetone and acetaldehyde were also slightly above zero.

Air temperatures throughout the measurement period ranged from 4°C at night to a maximum of 32°C during the day and therefore allowed us to analyze temperature as a likely driver of the OVOC fluxes. All fluxes were aggregated into 2°C intervals. MBO fluxes were also analyzed for light dependence by aggregating fluxes measured at 25 ± 2°C into PAR intervals of 100 μmol m^{-2} s^{-1} (Figures 18a and 18b). MBO light and temperature responses were virtually identical to the leaf level measurements presented by *Harley et al.* [1998] for trees at the same site. The remarkable match implies that there were no major systematic errors in our canopy-scale flux measurements. The temperature response of canopy-scale MBO fluxes was slightly steeper than measured from the leaf level and was more so if leaf temperatures were used instead of air temperature (data not shown). However, since no tower flux data were obtained above 32°C, no systematic deviation from the published leaf level temperature response [*Harley et al.*, 1998] should

be inferred from our data. Mean daytime MBO fluxes reported here are approximately 35-40% higher than those measured using a different REA system at the same site over a much shorter period in July 1998 [*Baker et al*., 1999], and approximately 40-45% lower than fluxes measured using an above canopy gradient approach in at the site in July and August 1998 [*Schade et al*., 2000].

Leaf level MBO fluxes were also investigated by Dennis Gray from State University of New York, Stoneybrook in 1998 (reported in *Schade et al.,* 2000). He found that MBO emissions were significant from current year needles as soon as they were long enough to be clamped inside the leaf cuvette (~3.5 cm). Highest emissions were measured from current year and one-year old needles, and the mean maximum basal emission rate (emissions at 30°C and 1000 µmol m^{-2} s^{-1} PAR) was 18 µg C g^{-1} h^{-1}, which was significantly lower than the 25 µg C g^{-1} h^{-1} found by Harley et al. (1998). Basal emissions showed a seasonal cycle with a maximum in August when both ambient temperatures and ecosystem carbon uptake peaked. One-year-old needles showed slightly lower MBO emissions than current year needles, and two-year-old needles showed on average 50 % lower MBO emissions on a mass basis (Gray et al., in preparation).

Fluxes of MBO from western US pine species can, in general, be described in the same way as isoprene emissions from oak species. They show both light and temperature responses as discussed above. We have used these response functions to model MBO emissions from our ponderosa pine plantation, and developed a more detailed leaf emission model to account for the plantation's relatively open structure. Here, we further develop our ponderosa pine modeling approach: As described in *Schade et al.* [2000] we model emissions from an individual, representative ponderosa pine tree using its average LAI and biomass in three vertical layers consisting of the three age classes of needles the tree supports at this site (current year, one year, and two year old). Light is allowed to strike the tree from all sides. The sunlit portion of leaves is calculated from

$$L_{sunlit} = [1 - exp(-k \times L_p \times \Omega)] / k \qquad (2),$$

where L_p is the projected or one-sided leaf area index (total leaf area index divided by 3.3 for ponderosa pine [*Schade et al*., 2000]), k denotes the extinction coefficient and Ω is the within-shoot clumping factor. Ω was estimated to be 0.8 for the ponderosa pine trees

[*Goldstein et al*., 2000]. The extinction coefficient k equals 0.5/sin(B) for a spherical leaf angle distribution, with B being the solar elevation angle. Though there are indications for a more vertical distribution, we presumed a spherical distribution as is commonly done in VOC emission modeling [*Guenther et al.*, 1995]. Finally, L_p was calculated from the transect LAI estimates and the ponderosa pine ground coverage (40%).

The PAR incident on sunlit leaves was calculated from

$$PAR_{sunlit} = PAR_{direct} \times k + PAR_{shade} \quad (3).$$

The direct and diffuse components of PAR were calculated from total above canopy PAR and algorithms published by *Weiss and Norman* [1985]. Contrary to the model by *Guenther et al*. [1995], shade leaf PAR was estimated directly from above canopy diffuse PAR applying the "slab" method described by *Norman* [1979], and assuming a leaf reflectance of 0.08 [*Pu et al*., 1998] and a leaf transmittance of zero in the PAR wavelengths.

The MBO basal emission rate, ε, was adopted to be 18 μg g^{-1} h^{-1} from leaf level measurements carried out in 1998 (see above), and reported in *Schade et al*. [2000], and was scaled by leaf age. Thus, the model includes a plant physiological response, i.e. leaf age (90% and 50% of current year needle emissions assumed for one year and two year old needles, respectively). Instantaneous changes in the emission rate according to changes in the light and temperature environment were modeled based on air temperature at tree height, and above canopy PAR fluxes. Canopy scale fluxes, F_{MBO}, were calculated from

$$F_{MBO} = \varepsilon \times D \times \gamma \times \delta \times f \quad (4),$$

where γ represents the light and temperature emission parameters [*Schade and Goldstein*, 2001], D is biomass density, δ scales the emission to leaf age and potential biomass density changes, and f is the ponderosa pine ground coverage. The variation of the model input parameters is shown in Table 4. Note that the trees support a sizable amount of biomass at this age (≤10 years old) and that there was continuing growth during the measurement campaign in July and August 1999.

Major uncertainties using this approach are the light transmission model and the ponderosa pine ground coverage. The latter was found to be not uniform, showing a

higher tree density closer to the tower (<80 m) than further away from it (>150 m). In an attempt to improve the model estimate, we scaled both the ground coverage and LAI with the predictions of a fetch model (C.-I.. Hsieh, personal communication, 2000) and our transect measurements, which showed that most of the flux is expected to come from distances closer to the tower. However, both the scaled LAI and ground coverage used in the model presented here were only 5% larger then the average ponderosa pine ground coverage for the daytime fetch area. Minor uncertainties are associated with the leaf biomass, the age scaling of the basal emission rate, the emission parameters, and the mean emission potential of 18 $\mu g\ g^{-1}\ h^{-1}$ for current year needles.

Daytime fluxes were predicted extremely well by the model (r^2=0.91, slope = 1.02) except for a few outliers (Figure 19). The model emissions also predicted diurnal changes in the MBO emission rate well (Figure 20). However, actual emissions were slightly overestimated in the morning and slightly underestimated in the late afternoon.

Table 4. Input Parameters to the MBO Leaf Emission Model.

	$D \times \delta$ [a] ($g\ m^{-2}$)	$LAI \times \delta$ [b] ($m^2\ m^{-2}$)	f	$\varepsilon \times \delta$ ($\mu g\ g^{-1}\ h^{-1}$)
Age 0	70-155 [c]	0.7-1.55 [c]	0.4	18
Age 1	150	1.25	0.4	16.2
Age 2	120	1	0.4	9
Error	10%	10%	10%	5%

[a] based on the area the tree covers
[b] all-sided LAI (divide by 3.3 for projected LAI)
[c] (non-linear) increase during the measurement period (specific leaf area is 100 $g\ m^{-2}$ for current year needles, and 120 $g\ m^{-2}$ for one- and two-year old needles).

4.2.1.2 Other Oxygenated VOCs

Flux dependencies on temperature for the other OVOCs were analyzed on the basis of the inferred algorithm

$$F_{OVOC} = F_{ref} \exp [\beta \times (T - T_{ref})] \quad T_{ref} = 303 \text{ K} . \qquad (5)$$

Beta factors and fluxes at 303 K were calculated from trimmed logarithmic regressions to the aggregated data, and are summarized in Table 5. The data and curves for the OVOC temperature responses are shown in Figures 21 and 22.

Table 5. Emission Factors for the Canopy and Bare Soil (O)VOC Emissions.

	Canopy-scale Emissions			Soil Emissions[a]	
	F_{ref}[b]	β	r^2	β	r^2
Methanol	2.87	0.11	0.94	0.03	0.70
Ethanol	0.64	0.14	0.86	NA[c]	NA
Acetone	0.37	0.11	0.98	0.02	0.78
Acetaldehyde	0.20	0.13	0.92	0.05	0.96
α-pinene	0.19	0.12	0.91	NA[c]	NA

[a] Based on topsoil temperatures.
[b] In mg C m^{-2} h^{-1} (at 30 °C).
[c] No systematic variation with temperature (ethanol), or no emissions (α-pinene).

4.2.1.3 Flux Measurement Error Estimate

The overall error in *F* was estimated from (1) as follows: Assuming a relative uncertainty in the determination of s_w and *b* of a maximum of 10% each, the total error for an individual flux measurement is dominated by the OVOC mixing ratio measurement accuracy in the updrafts and downdraft samples. Except for methanol, which coeluted with MEK and 3-methyl-furan, the precision for each compound, based on multiple calibration lines, was better then 10%, and the overall accuracy, including random errors computed from channel intercomparisons, was better than 15%. Therefore, the total random error for a single flux measurement was less than 25%. Higher errors have to be inferred for methanol because of its occasional abundance in blank samples [*Lamanna and Goldstein*, 1999] and the uniform correction of its mixing ratios applied to each individual sample. On the basis of the latter the potential systematic error for the

methanol fluxes was estimated from the error of the acetone to MEK correlation measured in July 1997 and June 1999 ($r^2 > 0.9$) plus the error in the 3-methyl-furan yield from isoprene (± 35%) to be 30-55% (median to 0.9 quantile) at most. The mean and maximum relative corrections applied were approximately 10% and 30% of both channels, dominantly inferred from MEK.

4.2.2 Monoterpenes

Monoterpene fluxes are driven mostly by temperature [*Tingey et al*., 1980; *Guenther et al*., 1993; *Fall*, 1999], including those from ponderosa pine [*Lerdau et al*., 1994]. Monoterpene fluxes have been measured at the canopy scale by gradient flux [e.g. *Schade et al.*, 1999b; *Rinne et al.*, 2000a], REA flux [e.g. *Christensen et al.*, 2000; *Gallagher et al.*, 2000; *Valentini et al.*, 1997], and disjunct eddy sampling methods [*Rinne et al.*, 2000b], all through collecting samples on cartridges for discrete periods with later analysis in the laboratory, but our measurements are the first using an REA system coupled to an automated in-situ GC for longer term continuous measurements. The temperature response of the pinene fluxes measured at our site is shown in Figure 23. It follows an exponential curve with beta-factors of approximately 0.12. However, extreme dryness or wetness can trigger lower or higher than expected emissions based on the temperature response only [*Schade et al*., 1999b]. Such extremes can be experienced in Mediterranean type ecosystems such as the Sierra Nevada Mountains. Prolonged summer dryness can lead to drought stress. Drought-stressed ecosystems exchange less latent heat compared to sensible heat, which can lead to extremely low ambient humidity levels.

In summer 1999 at Blodgett Forest, no such extreme events as in 1998 were observed. However, pinene fluxes slightly higher than expected fluxes were observed after a minor rain event (see 4.1.3), and slightly lower than expected fluxes during two days preceding the rain event when relative humidity levels had dropped below 20% during the day (responsible for the higher variability at the highest temperatures).

Due to smaller fluxes of the monoterpenes, a lower detectability and accuracy is achieved compared to MBO. To improve this in the future, we intend to increase the

current sample size and modify the sampling procedure in order focus on the monoterpene mixing ratios and fluxes, and their role in secondary aerosol formation.

4.3 Soil and Litter (O)VOC Flux Investigations

We carried out a limited number of chamber flux measurements on “bare soil”, “soil plus litter”, and “only litter”, mostly under completely dry conditions for both the soil and litter compartments. In general, similar OVOC distributions were encountered in all enclosure samples compared to the atmosphere. OVOCs clearly dominated the emissions, as demonstrated before by *Warneke et al.* [1999]. The main OVOCs emitted were acetone, acetaldehyde, and methanol or MEK (as we do not have soil emission measurements on a column other than the Rtx-WAX, we cannot assess how much of the methanol peak was actually MEK). Smaller emissions were observed for ethanol, isopropanol (tentatively), pentanal, hexanal, butanal, and three unidentified compounds. No monoterpenes were emitted from bare soil, but fresh ponderosa pine litter emitted large quantities of monoterpenes as an exponential function of temperature (data not shown); 1 year old litter still emitted monoterpenes but at much lower levels. However, neither fresh nor old ponderosa pine litter had large OVOC emissions, in contrast to leaf litter from manzanita bushes, which exhibited large emissions of acetaldehyde and methanol.

Figure 24 shows acetone emissions measured throughout the summer from two different soil locations. Fluxes depended on topsoil temperature and were lower than bare soil fluxes in cases where the ponderosa pine litter obviously shaded and cooled the soil beneath it. The range of temperatures shown in Figure 24 was commonly observed throughout the plantation. Bare soil surface temperatures in full sunlight routinely reached values higher than 60°C, and litter layer temperatures, also in full sunlight, higher than 55°C.

Two points, which showed enhanced soil OVOC emissions, have been omitted from Figure 24. These occurred from a wetted soil surface after a minor rain event during the night of August 26-27, 1999. Acetone fluxes were a factor of 3-4 higher that morning compared to the data shown in Figure 24, while the increase in emissions of methanol

and acetaldehyde was smaller, though still prominent.

An overnight measurement of the major OVOCs emitted from the soil in October 1999 is shown in Figure 25. Methanol, acetaldehyde, and acetone were emitted throughout the night as inferred from their peak areas compared to chamber blanks, and all compounds showed a strong response to increasing topsoil temperatures after sunrise. Using all our flux measurements and topsoil temperature, we calculated β-factors for the major OVOC fluxes according to (2). They are included in Table 5 and are in general lower than the ones calculated from the canopy-scale REA flux measurements and air temperatures. That is likely due to the strong temperature gradients through the soil profile and our use of topsoil temperatures.

The soil chamber measurements shown in Figure 25 demonstrated that a small flux of methanol, acetaldehyde and acetone was maintained at night. Assuming that these OVOC fluxes were of biogenic origin, and would therefore probably have a compensation point (such as found, for example, for ammonia [*Schjoerring et al*., 1998]), they could be an artifact due to the use of zero air in the chamber tests. If the measured fluxes were of nonbiogenic origin, we can infer that the measured nighttime canopy-scale fluxes discussed above were real. For ethanol, nighttime fluxes may be dominated by the ponderosa pine trees, as ethanol emissions from the soil were very low. The picture is less clear for methanol because of its high variability and the possible systematic error in its flux determination due to its coelution with MEK.

It is clear from these results that a significant percentage of the total fluxes could have derived from the on-site soil and litter. In particular, the underbrush clearing in June 1999 left large amounts of manzanita litter on the ground, which probably contributed especially to the methanol, acetaldehyde, and acetone fluxes. However, as shown by our bare soil flux tests, large amounts of litter were not a necessary requirement for OVOC emissions. We estimate that if the average topsoil temperature in the fetch area during daytime was between 30° and 50°C, 20-40% of the methanol, 30-45% of the acetone, and 20-65% of the acetaldehyde canopy-scale emissions could have come from the soil. The relative contribution probably changed when the soil got wet from rain or dew, as occurred during August 26-27, 1999: As shown in Figure 26, the acetone fluxes increased

dramatically during the rain. The following morning, when the topsoil was still wet, canopy-scale acetone fluxes were elevated, and soil acetone fluxes were elevated compared to dry soil samples, though the soil temperatures were similar to those of the days before. Fluxes of methanol and acetaldehyde were also elevated during the rain event but much less so compared to acetone. As the canopy-scale fluxes during the rain were consistent with the results from the respective chamber tests the next morning, we infer that the increase in emissions was mainly a result of wetting the soil surface. The effect of wetting as well as the dominance of acetone in the OVOC soil emissions are very similar to the results of *Warneke et al*. [1999] but had not been shown under field conditions before. We also note that our observed fluxes of pentanal and hexanal correspond to the masses 87 and 101 measured by *Warneke et al.* [1999].

5. Implications and Conclusions

Oxygenated VOCs make up a major part of atmospheric reduced carbon in the Sierra Nevada Mountains, and the emissions of these OVOCs are predominantly of natural origin. However, the relative impact of biogenic and anthropogenic emissions was different for each individual OVOC. That difference was also apparent in the flux data, showing higher emissions for MBO and methanol than for ethanol or the carbonyls.

MBO emissions were completely of biogenic origin, and the dependence of emissions on temperature and light agree very well with the responses previously published by *Harley et al*. [1998]. However, comparing our own measurements to a detailed leaf emission model [*Schade et al.*, 2000; *Schade and Goldstein*, submitted to JGR] suggests that the mean "basal emission rate" (emissions at 30 °C and 1000 µmol m^{-2} s^{-1} PAR) of ponderosa pine is most likely smaller than 20 µg g^{-1} h^{-1}, more than 20% lower than given by *Harley et al*. [1998]. Furthermore, similar to the isoprene basal emission rate [*Geron et al*., 2000], the MBO basal emission rate also shows a seasonal [*Schade et al*., 2000], and diurnal [*Schade and Goldstein*, submitted to JGR] change following ambient weather conditions. During and after hot days, the potential for MBO emission can be up to 50% higher than expected. This should be kept in mind when analyzing high ozone episodes in summer in relation to biogenic hydrocarbon emissions.

Methanol was emitted from the pine ecosystem at a rate similar to MBO, but anthropogenic methanol emissions also significantly affected observed mixing ratios. Assuming that similar flux magnitudes are confirmed in other ecosystems, methanol emissions must be considered a major VOC emission and a significant plant carbon loss on a global basis [*Guenther et al.*, 1995], yet they are not likely to be important for local or regional photochemical ozone formation. In comparison, fluxes of ethanol may not be as significant globally, because not all tree species are considered to be high ethanol producers, like ponderosa pine. However, both ethanol and methanol oxidation in the atmosphere lead to the production of aldehydes that can be photolyzed and can therefore contribute to HO_x production. Because of their lifetimes, effects of ethanol emissions on HO_x chemistry would be mostly regional whereas methanol is transported globally and to the upper troposphere, where its effects on HO_x may be substantial and more widespread

[*Singh et al.*, 1995]. As a possibly significant source of acetaldehyde and, subsequently, PAN, ethanol may also play a significant role in the long-range transport of NO_x. In addition, because ethanol is now being widely used as a fuel additive in California, it is useful to understand the magnitude of biogenic emissions for this compound in order to put the new anthropogenic emissions from fuel use into perspective, and it may therefore be worthwhile to study ethanol emissions from other ecosystems in the future.

Monoterpenes were observed to be solely of biogenic origin, and fluxes from ponderosa pine at the Blodgett Forest site were mainly driven by temperature, as described before [*Lerdau et al*., 1994]. Humidity has a secondary effect on monoterpene fluxes that comes into play during extreme events, such as summer rain storms or prolonged summer droughts, both comparatively common to the Mediterranean climate of the Sierra Nevada mountains. In view of its potential impact on secondary aerosol formation, it is worthwhile to further study this effect, including different plant species and how ambient humidity levels may change both the amount and composition of emitted monoterpenes. It is also worthwhile to further study the emission rates of the less abundant monoterpenes because it is really the sum of all monoterpenes that causes secondary aerosol formation.

Acetone was observed to be of both biogenic and anthropogenic origin, and fluxes measured from this ponderosa pine plantation leave us with many interesting questions. There are only a few published reports on acetone emissions in addition to our own work. One focused on leaf surface ozonolysis as the main source of acetone [*Fruekilde et al.*, 1998]. We analyzed our acetone flux data in search of a relation to either ozone mixing ratios or measured ozone deposition [*Bauer et al.*, 2000] but found no evidence for a possible connection to either. Nevertheless, assuming no other significant live plant sources at our site besides ponderosa pine, the trees still contributed more than 50% to the canopy-scale fluxes (daytime: 0.23-0.39 $\mu g\ g^{-1}\ h^{-1}$). The leaf level fluxes reported by *Martin et al*. [1999] and *Janson et al*. [1999] for a number of spruce, fir, and pine species were similar to this range, which implies that acetone emissions are a common feature at least among the coniferous species. However, as there is little knowledge as to how acetone is produced inside the leaves, what regulates its emissions, and how much is

emitted on a day-to-day basis [*Fall*, 1999], more research is needed in this area. We present canopy-scale acetone fluxes and show that temperature was the main regulating parameter. At times, acetone fluxes may be dominated by soil and litter emissions, which were clearly elevated by wetting. *Warneke et al* [1999] demonstrated that Maillard-type reactions can produce large amounts of acetone in decaying organic matter by a process of heating and wetting. Such processes can occur especially in Mediterranean-, savanna-, and grassland-type ecosystems, possibly also in tropical rain forests. In the Sierra Nevada, where little rain falls in summer, the first rain in fall might produce a large pulse of acetone, and we have shown the effect in Figure 26.

In summary, the emissions of oxygenated VOCs, largely underrepresented in field and laboratory measurements so far, are a substantial component of total biogenic VOC fluxes. Our measurements, and the analytical tools we have developed, will allow improvement of estimates of their emissions globally [*Guenther et al.*, 1995] and in California (using BEIGIS), but more laboratory and field measurements in other ecosystems are necessary before broad-scale conclusions should be drawn. Also, more investigations into litter and soil emissions are needed to determine which ecosystem components are dominating emissions and how they respond to environmental drivers.

Oxidation of isoprene in the boundary layer contributes substantially to regional ozone production in the Sierra Nevada Mountains. Our estimates indicate that, on average, approximately 50% of the ozone produced during upslope daytime flow is associated with biogenic isoprene oxidation in summer. During hot days with maximum temperatures exceeding 30 °C, virtually all ozone produced may be associated with isoprene oxidation. Although this analysis is based on a number of assumptions about chemistry and transport between the Sierra Nevada foothills and our measurement site, we conclude that summertime high ozone levels throughout mid level elevations of the Sierra Nevada east of Lake Tahoe are fueled by biogenic hydrocarbon emissions, in particular isoprene. Significant reductions of these high ozone levels can therefore not be achieved by reducing anthropogenic hydrocarbon emissions in the upwind area, but would rather have to be achieved by significantly reducing anthropogenic NO_x emissions from mobile sources in the Sacramento Valley.

6. References

Apel, E.C., J.G. Calvert, J.P. Greenberg, D. Riemer, R. Zika, T.E. Kleindienst, W.A. Lonneman, K. Fung, and E. Fujita, Generation and validation of oxygenated volatile organic compound standards for the 1995 Southern Oxidants Study Nashville Intensive, *J. Geophys. Res.*, *103*(D17), 22,281-22,294, 1998.

Arey, J., A.M. Winer, R. Atkinson, S.M. Aschmann, W.D. Long, C.L. Morrison, and D.M. Olszyk, Terpenes emitted from agricultural species found in California's central valley, *J. Geophys. Res.*, 96, 9329-9336, 1991.

Baker, B., A. Guenther, J. Greenberg, A. Goldstein, and R. Fall, Canopy fluxes of 2-methyl-3-buten-2-ol over a ponderosa pine forest by relaxed eddy accumulation: Field data and model comparison, *Journal of Geophysical Research, 104* (D21), 26107-26114, 1999.

Bauer, M.R., J.A. Panek, N.E. Hultman, A.H. Goldstein, Ozone deposition to a ponderosa pine plantation in the Sierra Nevada Mountains (CA): a comparison of two different climatic years, *J. Geophys. Res.*, *105*(D17), 22,123-22,136, 2000.

Biesenthal, T.A., Q. Wu, P.B. Shepson, H.A. Wiebe, K.G. Anlauf, G.I. Mackay, A study of relationships between isoprene, its oxidation products, and ozone, in the Lower Fraser Valley, BC., *Atmos. Environ.*, *31*(14), 2049-2058, 1997.

Bowling, D.R., A.A. Turnipseed, A.C. Delany, D.D. Baldocchi, J.P. Greenberg, and R.K. Monson, The use of relaxed eddy accumulation to measure biosphere-atmosphere exchange of isoprene and other biological trace gases, *Oecologia, 116*, 306-315, 1998.

Chameides, W.L., R.W.Lindsay, J. Richardson, and C.S. Kiang, The role of biogenic hydrocarbons in urban photochemical smog: Atlanta as a case study, *Science*, 241, 1473-1475, 1988.

Christensen, C.S., P. Hummelshoj, N. O. Jensen, B. Larsen, C. Lohse, K. Pilegaard, and H. Skov, Determination of the terpene flux from orange species and Norway spruce by relaxed eddy accumulation, *Atmospheric Environment*, 34 (19), 3057-3067, 2000.

Delon, C., A. Druilhet, R. Delmas, and J. Greenberg, Aircraft assessment of trace compound fluxes in the atmosphere with Relaxed Eddy Accumulation: Sensitivity to the conditions of selection, *Journal of Geophysical Research, 105* (D16), 20461-20472, 2000.

Fall, R., Biogenic emissions of volatile organic compounds from higher plants, in *Reactive Hydrocarbons in the Atmosphere*, edited by C.N. Hewitt, pp. 41-96, Academic, San Diego, Calif.,1999.

Fehsenfeld, F., *et al*., Emissions of volatile organic compounds from vegetation and the implications for atmospheric chemistry, *Global Biogeochem. Cycles*, 6, 389-430,1992

Frost, G.J., et al., Photochemical ozone production in the rural southeastern United States during the 1990 Rural Oxidants in the Southern Environment (ROSE) program, *J. Geophys. Res.*, *103*(D17), 22,491-22,508, 1998.

Fruekilde, P., J. Hjorth, N.R. Jensen, D. Kotzias, and B. Larsen, Ozonolysis at vegetation surfaces: A source of acetone, 4-oxopentanal, 6-methyl-5-hepten-2-one, and geranyl acetone in the troposphere, *Atmos. Environ.*, *32*(11), 1893-1902, 1998.

Fuentes, J.D., D. Wang, G. Den Hartog, H.H. Neumann, T.F. Dann, and K.J. Puckett, Modelled and field measurements of biogenic hydrocarbon emissions from a Canadian deciduous forest, *Atmos. Environ.*, 29, 3003-3017, 1995.

Gallagher, M.W., R. Clayborough, K. M. Beswick, C. N. Hewitt, S. Owen, J. Moncrieff, and K. Pilegaard, Assessment of a relaxed eddy accumulation for measurements of fluxes of biogenic volatile organic compounds: study over arable crops and a mature beech forest, *Atmos. Environ.*, 34 (18), 2887-2899, 2000.

Geron, C., A. Guenther, T. Sharkey, and R.R. Arnts, Temporal variability in basal isoprene emission factor, *Tree Physiol.*, 20, 799-805, 2000.

Goldan, P.D., W.C. Kuster, F.C. Fehsenfeld and S.A. Montzka, The observation of a C5 alcohol emission in a North American pine forest, *Geophys. Res. Lett.*, 20, 1039-1042, 1993.

Goldan, P.D., W.C. Kuster, F.C. Fehsenfeld, and S.A. Montzka, Hydrocarbon Measurements in the Southeastern United States - the Rural Oxidants in the Southern Environment (ROSE) Program 1990, *J. Geophys. Res.*, *100*(D12), 25,945-25,963, 1995.

Goldstein, A.H., Daube, B.C., Munger, J.W., Wofsy, S.C., Automated in-situ monitoring of atmospheric non-methane hydrocarbon concentrations and gradients, *J. Atmos. Chem.*, 21, 43-59, 1995.

Goldstein, A. H., S.M. Fan, M.L. Goulden, J.W. Munger, S.C. Wofsy, Emissions of ethene, propene and 1-butene by a midlatitude forest, *J. Geophys. Res.*, 101, 9149-9157, 1996.

Goldstein, A. H., M.L. Goulden, J.W. Munger, S.C. Wofsy, and C.D. Geron, Seasonal Course of Isoprene Emissions from a Midlatitude Deciduous Forest, *J. Geophys. Res.*, V. 103, 31,045-31,056, 1998.

Goldstein, A.H., and G.W. Schade, Quantifying biogenic and anthropogenic contributions to acetone mixing ratios in a rural environment, *Atmos. Environ.*, *34*(29-30), 4997-5006, 2000.

Goldstein, A.H., N.E. Hultman, J.M. Fracheboud, M.R. Bauer, J.A. Panek, M. Xu, Y. Qi, A.B. Guenther, and W. Baugh, Effects of climate variability on the carbon dioxide, water, and sensible heat fluxes above a ponderosa pine plantation in the Sierra Nevada (CA), *Agric. For. Meteorol.*, *101*, 113-129, 2000.

Guenther, A.B., R.K. Monson, and R. Fall, Isoprene and monoterpene emission rate variability: Observations with eucalyptus and emission rate algorithm development, *J. Geophys. Res.*, *96*, 10799-10808, 1991.

Guenther, A.B., et al, A global model of natural volatile organic compound emissions. *J. Geophys. Res.*, *100*(D5), 8873-8892, 1995.

Guenther, A., W. Baugh, K. Davis, G. Hampton, P. Harley, L. Klinger, P. Zimmerman, E. Allwine, S. Dilts, B. Lamb, H. Westberg, D. Baldocchi, C. Geron, and T. Pierce, Isoprene fluxes measured by enclosure, relaxed eddy accumulation, surface-layer gradient, mixed-layer gradient, and mass balance techniques, *J. Geophys. Res.*, *101*, 18555-18568, 1996.

Harley, P., V. Fridd-Stroud, J. Greenberg, A. Guenther, and P. Vasconcellos, Emission of 2-methyl-3-buten-2-ol by pines: A potentially large natural source of reactive carbon to the atmosphere, *J. Geophys. Res.*, 103, 25,479-25,486, 1998.

Heck, W.W., and C.S. Brandt, Effects on vegetation: native crops, forest, *Air Pollution*, Vol. II, 157-229, Academic Press, London, 1977.

Isodorov, V.A., I.G. Zenkevich, and B.V. Ioffe, Volatile organic compounds in the atmosphere of forests, *Atmos. Environ.*, *19*, 1-8, 1985.

Janson, R., C. De Serves, and R. Romero, Emission of isoprene and carbonyl compounds from a boreal forest and wetland in Sweden, *Agric. For. Meteorol.*, *98-99*, 671-681, 1999.

Juuti, S. J. Arey, and R. Atkinson, Monoterpene emissions rate measurements from a Monterey pine, *J. Geophys. Res.*, *95*(D6), 7515-7519, 1990.

Kesselmeier, J.K., K. Bode, U. Hofmann, H. Müller, L. Schäfer, A. Wolf, P. Ciccioli, E. Brancaleoni, A. Cecinato, M. Frattoni, P. Foster, C. Ferrari, V. Jacob, J.L. Fugit, L. Dutaur, V. Simon, and L. Torres, The BEMA Project: Emission of short-chained organic acids, aldehydes, and monoterpenes, from *Quercus ilex* L. and *Pinus pinea* L. in relation to physiological activities, carbon budget and emission algorithms, *Atmos. Env*., *31*, 119-133, 1997.

Khalil, M.A.K., and R.A. Rasmussen, Forest hydrocarbon emissions: Relationships between fluxes and ambient concentrations, *J. Air & Water Man. As.*, *42*, 810-813, 1992.

Knoeppel, H., B. Versino, H. Schlitt, A. Peil, H. Schauenburg, and H. Visseres, Organics in Air. Sampling and Identification, in *Prod. 1st Eur. Symp. Physico-chemical behaviour of atmospheric pollutants*, edited by B. Versino and H. Ott. EUR 6621, Brussels, pp. 25-40, 1980.

Knoerr, K.R., and F.L. Mowry, Energy balance/Bowen ratio techniques for estimating hydrocarbon fluxes, in *Atmospheric Biogenic Hydrocarbons*, edited by J.J. Bufalini and R.R. Arnts, pp. 35-52, Butterworth, Stoneham, MA, 1981.

König, G., M. Brunda, H. Puxbaum, C.N. Hewitt, S.C. Duckham, and J. Rudolph, Relative contribution of oxygenated hydrocarbons to the total biogenic VOC emissions of selected mid-European agricultural and natural plant species, *Atmos. Environ*., 29, 861-874, 1995.

Lamanna, M.S., and A.H. Goldstein, *In-situ* Measurements of C_2-C_{10} VOCs Above a Sierra-Nevada Ponderosa Pine Plantation, *J. Geophys. Res.*, *104*(D17), 21,247-21,262, 1999.

Lamb, B., H. Westberg, and G. Allwine, Biogenic hydrocarbon emissions from deciduous and coniferous trees in the United States, *J. Geophys. Res.*, *90*, 2380-2390, 1985.

Lamb, B., H. Westberg, and G. Allwine, Isoprene emission fluxes determined by an atmospheric tracer technique, *Atmos. Environ.*, *20*, 1-8, 1986.

Lenschow, D.H., and M.R. Raupach, The attenuation of fluctuations in scalar concentrations through sampling tubes, *J. Geophys. Res.*, *96*(D8), 15,259-15,268, 1991.

Lerdau, M., S.B. Dilts, H. Westberg, B.K. Lamb, and E.J. Allwine, Monoterpene Emission From Ponderosa Pine, *J. Geophys. Res.*, *99* (D8), 16609-16615, 1994.

Martin, R.S., I. Villanueva, J. Zhang, and C.J. Popp, Nonmethane hydrocarbon, monocarboxylic acid, and low molecular weight aldehyde and ketone emissions from vegetation in central New Mexico, *Env. Sci. Technol*., *33*(13), 2186-2192,

1999.
McKeen, S.A., E.Y. Hsie, and S.C. Liu, A study of the dependence of rural ozone on ozone precursors in the eastern United States, *J. Geophys. Res.*, *96*, 15377-15394, 1991.
Monson, R.K., and R. Fall, Isoprene emission from aspen leaves: Influence of environment and relation to photosynthesis and photorespiration, *Plant Physiol.*, *90*, 267-274, 1989.
Montzka, S.A., M. Trainer, P.D. Goldan, W.C. Kuster, F.C. Fehsenfeld, Isoprene and its oxidation products, methyl vinyl ketone and methacrolein, in the rural troposphere, *J. Geophys. Res.*, *98*, 1101-1111, 1993.
Montzka, S.A., M. Trainer, W.M. Angevine, F.C. Fehsenfeld, Measurements of 3-methyl furan, methyl vinyl ketone, and methacrolein at a rural forested site in the southeastern United States, *J. Geophys. Res.*, *100*, 11393-11401, 1995.
National Research Council, Rethinking the Ozone Problem in Urban and Regional Air Pollution, Executive Summary, Washington D.C., National Academy Press, pp. 1-18, 1991.
Nemecek-Marshall, M., R.C. MacDonald, J.J. Franzen, C.L. Wojciechowski, and R. Fall, Methanol emission from leaves, *Plant Physiol.*, *108*(4), 1359-1368, 1995.
Nie, D., T.E. Kleindienst, R.R. Arnts, and J.E. Sickles, II, The design and testing of a relaxed eddy accumulation system, *J. Geophys. Res.*, 100, 11415-11423, 1995.
Nie, D., T. E. Kleindienst, R. R. Arnst, J. E. Sickles, *Correction to* The design and testing of a relaxed eddy accumulation system, *J. Geophys. Res.*, 101 (D2), 4315-4315, 1996.
Norman, J.M., Modeling the complete crop canopy. In: *Modification of the Aerial Environment of Crops*, edited by B.J. Barfield and G.F. Gerber, American Society of Agricultural Engineers, p. 249-277, 1979.
Oncley, S., A. Delany, T. Horst, and P. Tans, Verification of flux measurements using relaxed eddy accumulation, *Atmos. Environ.*, 27A, 2417-2426, 1993.
Ooy, D.J., and J.J. Carroll, The spatial variation of ozone climatology on the western slope of the Sierra Nevada, *Atmos. Environ.*, 29, 1319-1330, 1995.
Paulson, S.E. and J.H. Seinfeld, Development and evaluation of a photooxidation mechanism for isoprene, *J. Geophys. Res.*, 97, 20703-20715, 1992.
Pu, R. Xu, B., and P. Gong, Spectral analysis of conifer leaves at different ages, In: *Proceedings of the Geoinformatics '98 Conference "Spatial Information Technology Towards 2000 and Beyond"*, edited by Q. Zhou, H. Lin, and W. Shi, Beijing, China, p. 221-228, 1998.
Peterson, D.L., M.J. Arbaugh, V.A. Wakefield, and P.R. Miller, Evidence for growth reduction in ozone injured Jeffrey pine in Sequoia and Kings Canyon National Parks, *J. Air. Pollut. Control Ass.*, 37, 908-912, 1987.
Placet, M., et al., Emissions involved in acidic deposition processes, *NAPAP SOS/Tech. Rep. 1*, U.S. Government Printing Office, Washington, D.C., 1990.
Rasmussen, R.A., Isoprene identified as a forest type of emission to the atmosphere, *Environ. Sci. Tech.*, 4, 667-671, 1970.
Riemer, D., et al, Observations of nonmethane hydrocarbons and oxygenated volatile organic compounds at a rural site in the southeastern United States, *J. Geophys.*

Res., *103*(D12), 28,111-28,128, 1998.
Rinne, J., J.-P. Tuovinen, T. Laurila, H. Hakola, M. Aurela and H. Hypén, Measurements of hydrocarbon fluxes by a gradient method above a northern boreal forest. *Agricultural and Forest Meteorology*, 102, 25-37, 2000a.
Rinne, H. J. I., A. C. Delany, J. P. Greenberg & A. B. Guenther, A true eddy accumulation system for trace gas fluxes using disjunct eddy sampling method. *Journal of Geophysical Research*, 105, 24791-24798, 2000b.
Ruppert, L., and K.H. Becker, A product study of the OH radical-initiated oxidation of isoprene: Formation of C_5-unsaturated diols, *Atmos. Environ.*, *34*(10), 1529-1542, 2000.
Salardino, D.H., and J.J. Carroll, Correlation between ozone exposure and visible foliar injury in ponderosa and jeffrey pines, *Atmos. Env*., 32, 3001-3010, 1998.
Sanadze, G.A., The nature of gaseous substances emitted by leaves of Robina-pseudoacacia, *Soobshch. Akad. Nauk Gruz. SSR*, 19, 83-86, 1957.
Sanadze, G.A., Light-dependent excretion of molecular isoprene by leaves, *Prog. Photosyn. Res.*, *II*, 701-706, 1969.
Schade, G.W., R.M. Hofmann, and P.J. Crutzen, CO emissions from degrading plant matter, I: Measurements, *Tellus*, *Ser. B*, *51*, 889-908, 1999a.
Schade, G.W., A.H. Goldstein, and M.S. Lamanna, Are monoterpene emissions influenced by humidity?, *Geophys. Res. Lett.*, *26*(14), 2187-2190, 1999b.
Schade, G.W., A.H. Goldstein, D.W. Gray, and M.T. Lerdau, Canopy and leaf level emissions of 2-methyl-3-buten-2-ol from a ponderosa pine plantation, *Atmos. Env*., *34*(21), 3535-3544, 2000.
Schade, G.W. and A.H. Goldstein, Fluxes of oxygenated volatile organic compounds from a ponderosa pine plantation, *J. Geophys. Res*., 106(D3), 3111-3123, 2001.
Schere, K.L., Modeling ozone concentrations, *Envir. Sci. Technol.*, 22, 488-495, 1988.
Schjoerring, J.K., S. Husted, and M.M. Poulsen, Soil-plant-atmosphere ammonia exchange associated with *Calluna vulgaris* and *Deschampsia flexuosa*, *Atmos. Environ*., *32*(3), 507-512, 1998.
Singh, H.B., and P.B. Zimmerman, Atmospheric distributions and sources of nonmethane hydrocarbons, in *Gaseous Pollutants: Characterization and Cycling*, edited by J.O. Nriagu, 177-235, Wiley, New York, NY, 1992.
Singh, H.B., M. Kanakidou, P.J. Crutzen, and D.J. Jacob, High concentrations and photochemical fate of oxygenated hydrocarbons in the global atmosphere, *Nature*, *378*, 50-54, 1995.
Slemr, J., W. Junkermann, and A. Volz-Thomas, Temporal variations in formaldehyde, acetaldehyde and acetone and budget of formaldehyde at a rural site in Germany, *Atmos. Environ.*, *30*(21), 3667-3676, 1996.
Solberg, S., C. Dye, N. Schmidbauer, A. Herzog, and R. Gerhrig, Carbonyls and nonmethane hydro-carbons at rural European sites from the Mediterranean to the Arctic, *J. Atmos. Chem.*, *25*, 33-66, 1996.
Squillance, P.J., J.F. Pankow, N.E. Korte, and J.S. Zogorski, ,. Review of the environmental fate of methyl *tert*-butyl ether, *Env. Toxicol. Chem*., *16*(9), 1836-1844, 1997.
Stationary Source Division, Methyl Tert.-Butyl Ether, in *Toxic Air Contaminant*

Identification List Summaries, pp. 675-680, Air Resour. Board, Calif. Environ. Prot. Agency, Sacramento, Calif., 1997.

Tingey, D.T., M. Manning., L.C. Grothaus, and W.F. Burns, The influence of light and temperature on isoprene emission rates from live oak, *Physiol. Plant.*, *47*, 112-118, 1979.

Tingey, D.T., M. Manning, L.C. Grothaus, and W.F. Burns, Influence of light and temperature on monoterpene emission rates from slash pine, *Plant Physiol.*, 65, 797-801, 1980.

Trainer, M., E.J. Williams, D.D. Parrish, M.P. Buhr, E.J. Allwine, H.H. Westberg, F.C. Fehsenfeld, and S.C. Liu, Models and observations of the impact of natural hydrocarbons on rural ozone, *Nature*, 329, 705-707, 1987.

Valentini, R, S. Greco, G. Seufert, N. Bertin, P. Ciccioli, A. Cecinato, E. Brancaleoni, and M. Frattoni, Fluxes of biogenic VOC from Mediterranean vegetation by trap enrichment relaxed eddy accumulation, *Atmospheric Environment*, 31, 229-238, 1997.

Warneke, C., T. Karl, H. Judmaier, A. Hansel, A. Jordan, W. Lindinger, and P.J. Crutzen, Acetone, methanol, and other partially oxidized volatile organic emissions from dead plant matter by abiological processes: Significance for atmospheric HO_x chemistry, *Global Biogeochem. Cycles*, *13*, 9-17, 1999.

Weiss, A., and J.M. Norman, Partitioning solar radiation into direct and diffuse, visible and near-infrared components. *Agric. For. Meteorol*., *34*, 205-213, 1985.

Went, F.W., Air Pollution, *Sci. Am.*, 192, 63-72, 1955.

Winer, A., J. Arey, S. Aschman, R. Atkinson, W. Long, L. Morrison, and D. Olszyk, Hydrocarbon emissions from vegetation found in California's Central Valley, final report, *Calif. Air Resourc. Board contract A732-155*, Statewide Air Pollut. Res. Cent., Univ. of Calif., Riverside, 1989.

Xu, M., Ecosystem carbon measurement, modeling, and management in a young ponderosa pine plantation in northern California, *PhD thesis*, University of California, Berkeley, 2000.

Zhang, S.-H., M. Shaw, J.H. Seinfeld, and R.C. Flagan, Photochemical Aerosol Formation from α-pinene and β-pinene, *J. Geophys. Res.*, *97* (D18), 20717-20729, 1992

Zimmerman, P.R., Determination of emission rates of hydrocarbons from indigenous species of vegetation in the Tampa/St. Petersburg Fla. area, Final Appendix C, *Rep. EPA-904/9-77-028*, U.S. E.P.A., Research Triangle Park, NC, 1979.

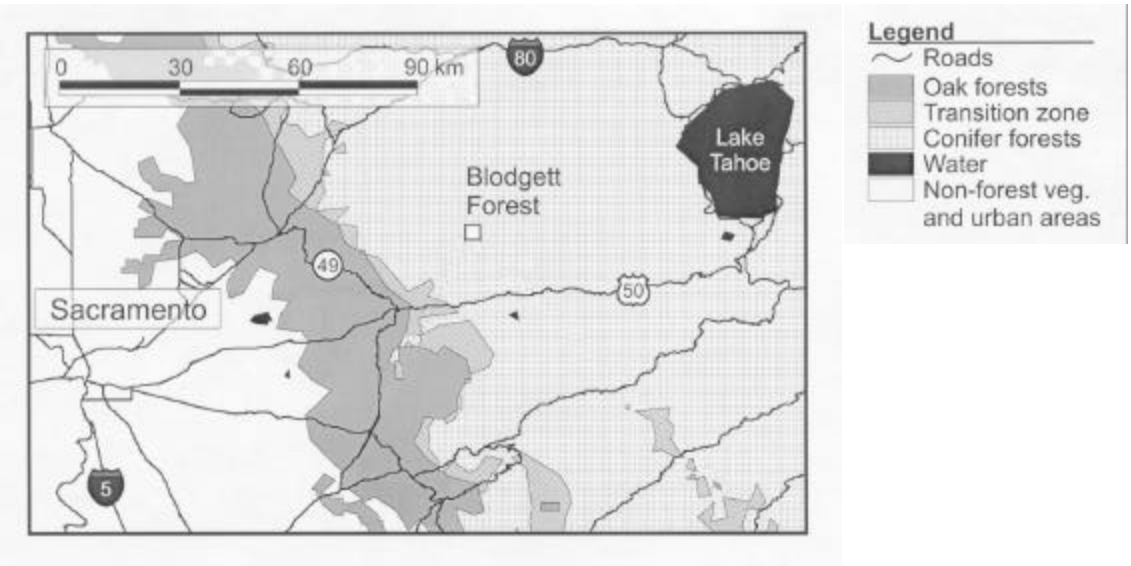

Figure 1. Map showing the regional setting and vegetation near the Blodgett Forest tower site. Vegetation distribution is derived from the USGS Seasonal Land Cover Regions classification, which is based on 1 km pixel AVHRR data. The "Oak Forests" category shown here comprises both oak forest and woodland areas [from Goldstein et al., 2000].

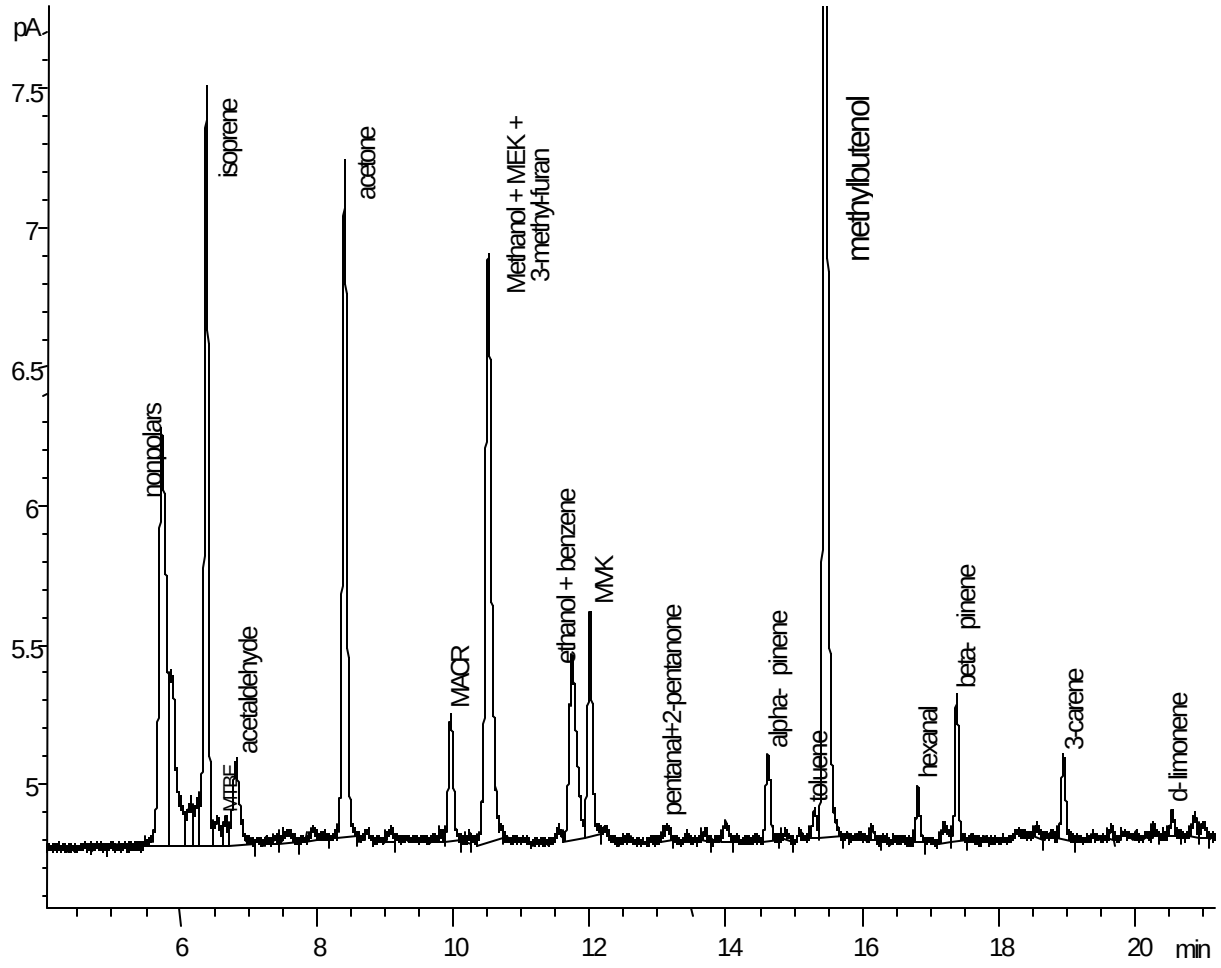

Figure 2. Sample chromatogram from the Rtx-WAX column (July 1999).

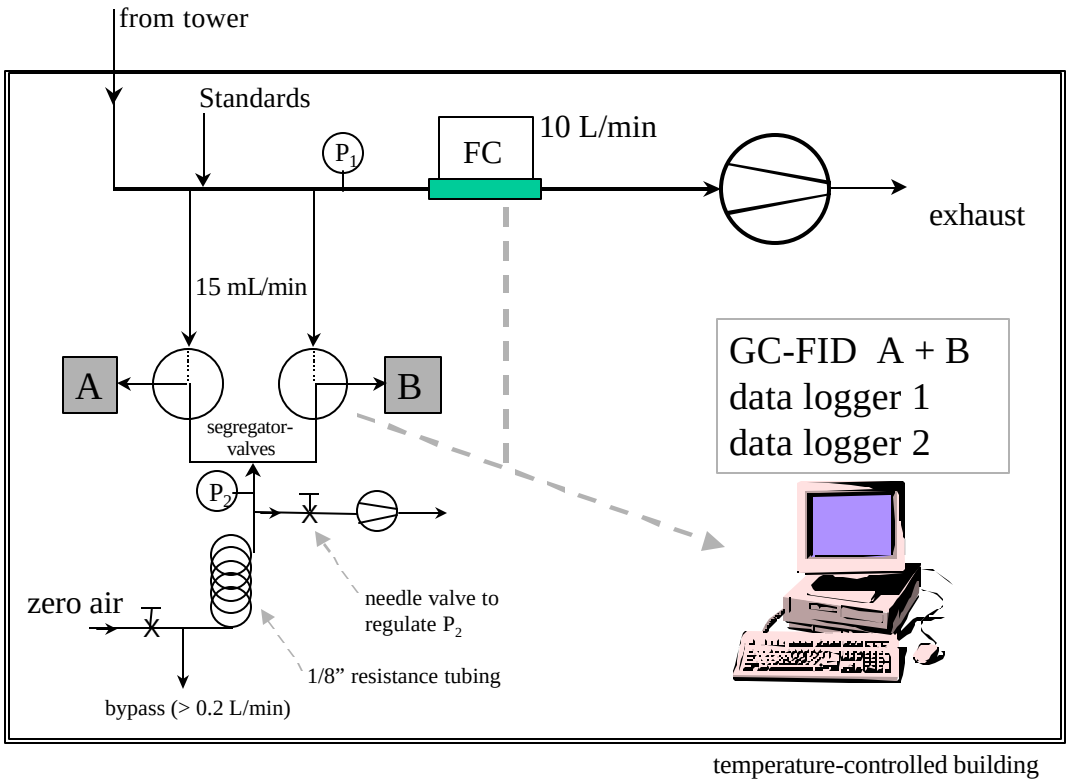

Figure 3. Schematic representation of the REA measurement setup. "A" and "B" represent the up and down samples leading to the two microtraps and GC-FID channels. "FC" stands for flow controller, and "P_1" and "P_2" are pressure sensors used to set the zero air pressure to the sampling line pressure as indicated.

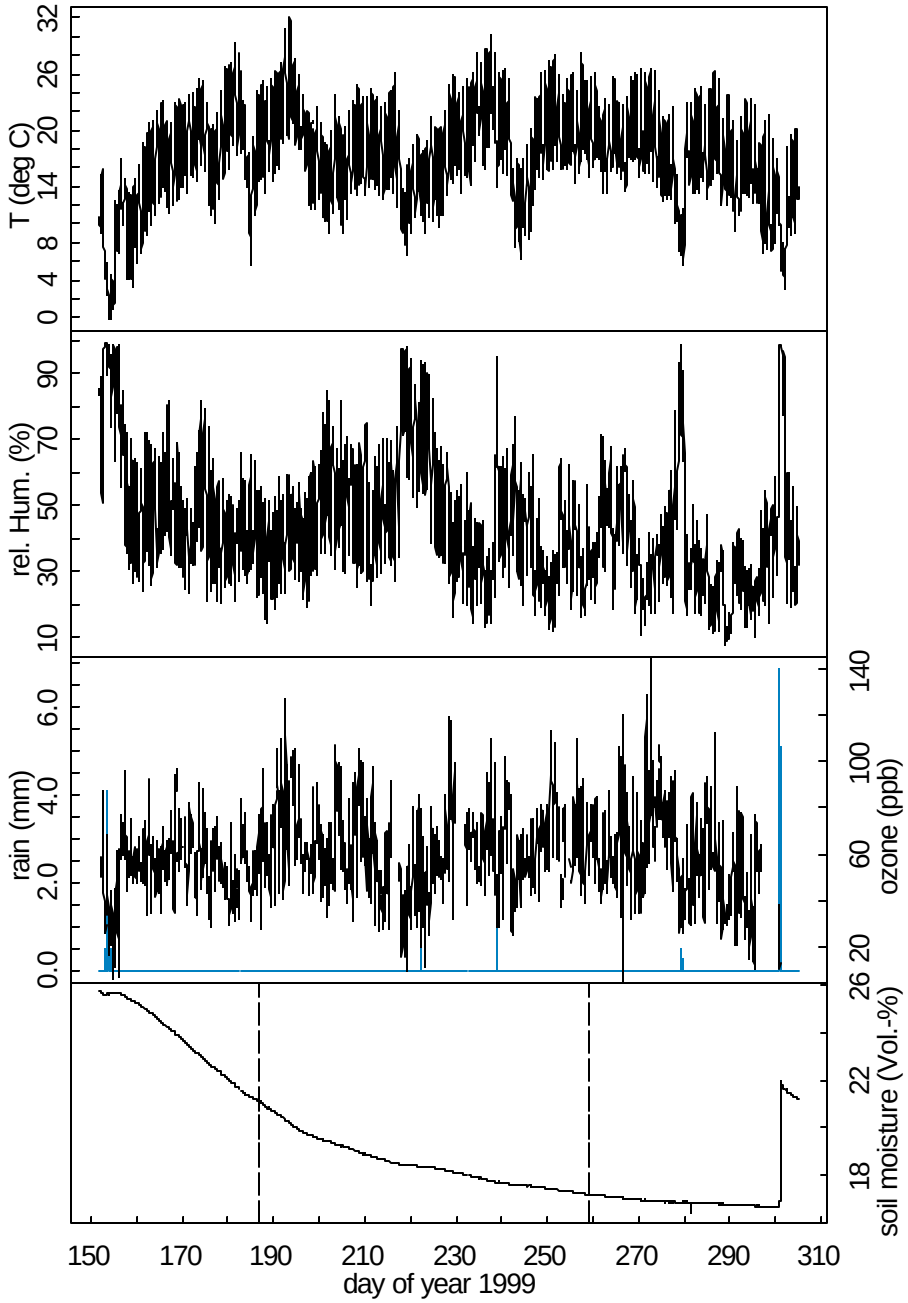

Figure 4. Meteorological parameters measured near Blodgett Forest Research Station from June to October 1999. The vertical dashed lines mark the period for which OVOC flux measurements are reported.

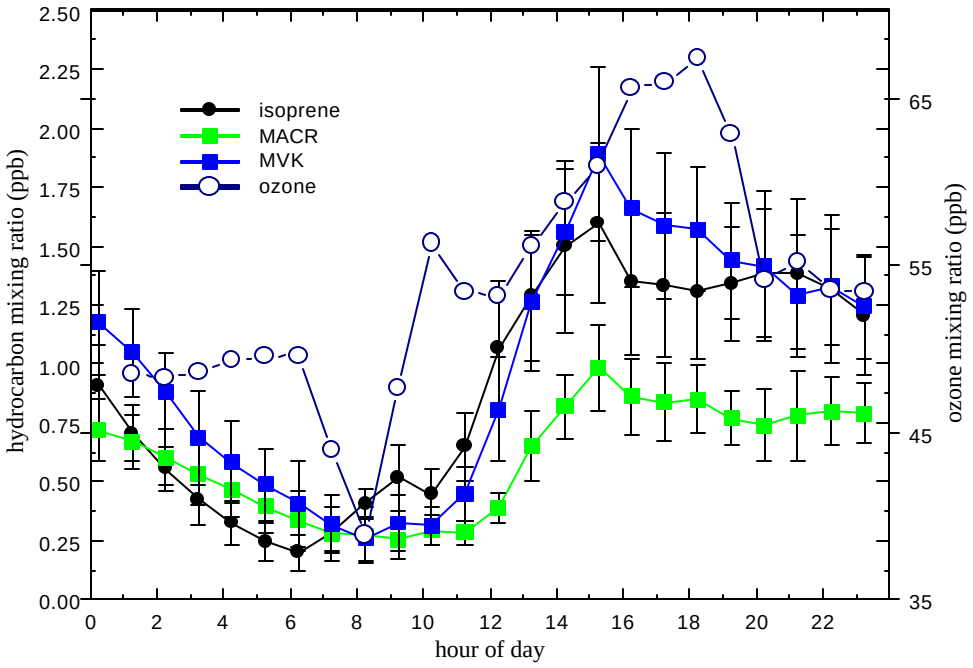

Figure 5. Mean diurnal cycle of Isoprene, its oxidation products methacrolein (MACR) and methyl vinyl ketone (MVK), and ozone during July 1998.

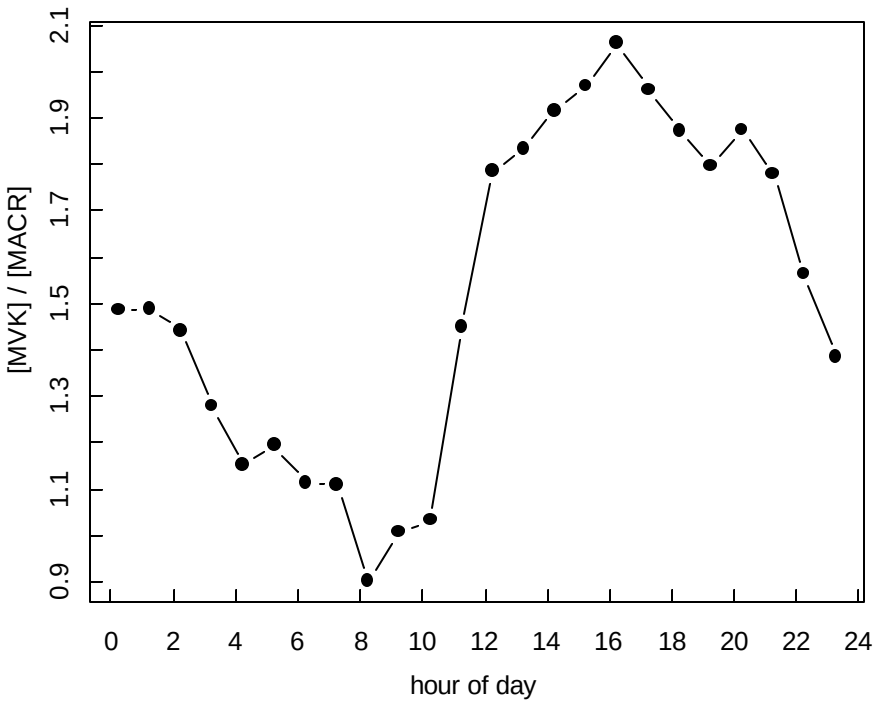

Figure 6. Mean diurnal cycle of the ratio of methyl vinyl ketone (MVK) to methacrolein (MACR) during July and August 1998.

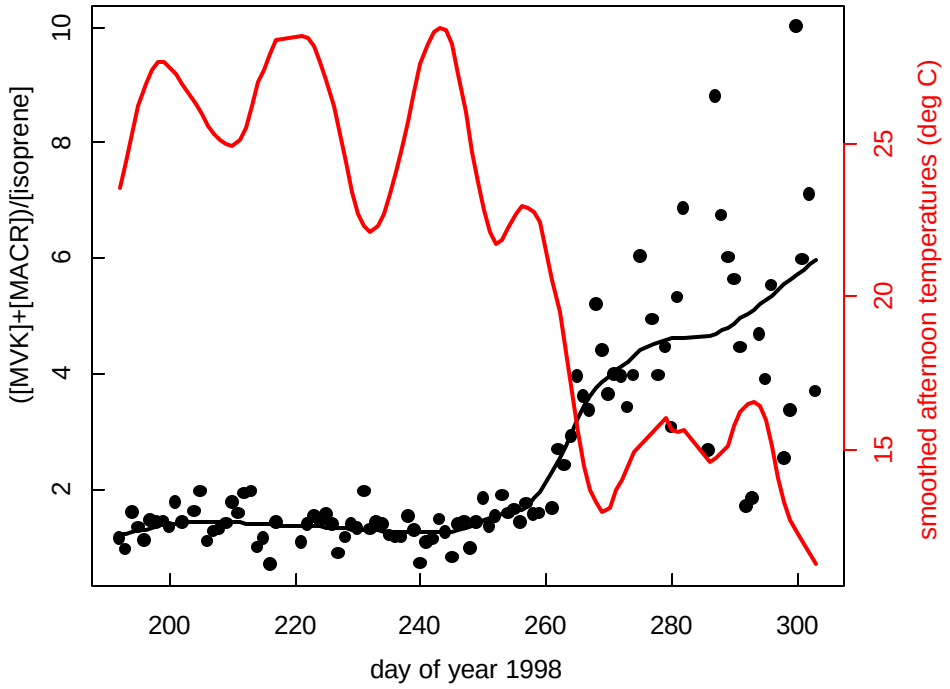

Figure 7. Seasonal cycle of the daytime ratio of methyl vinyl ketone (MVK) plus methacrolein (MACR) to Isoprene during July through October 1998. Smoothed mean afternoon temperature is shown in red.

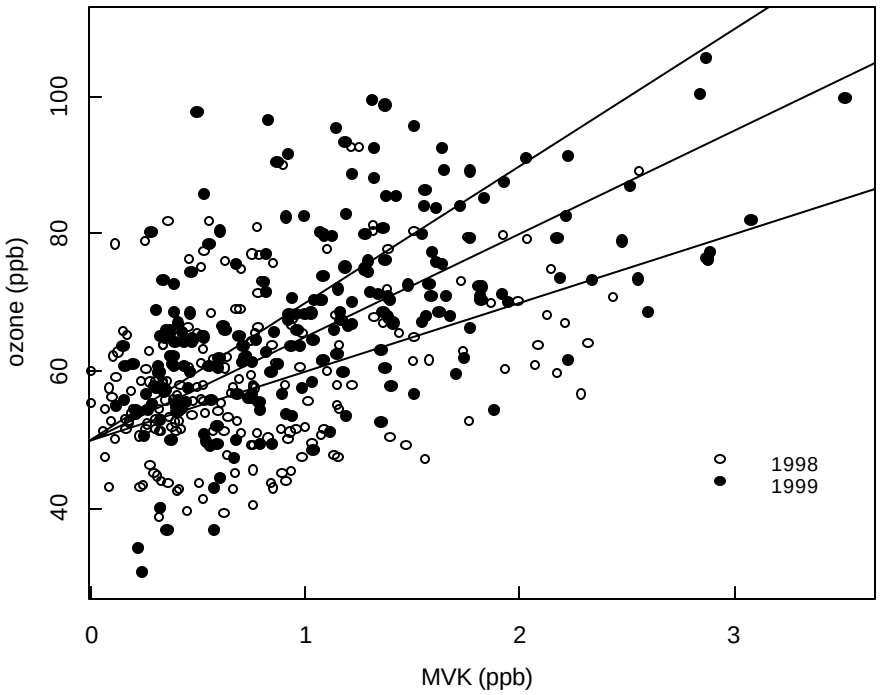

Figure 8. Methyl vinyl ketone (MVK) versus ozone mixing ratios from late morning through afternoon during the summers of 1998 and 1999. Lines indicate slopes of 10, 15, and 20.

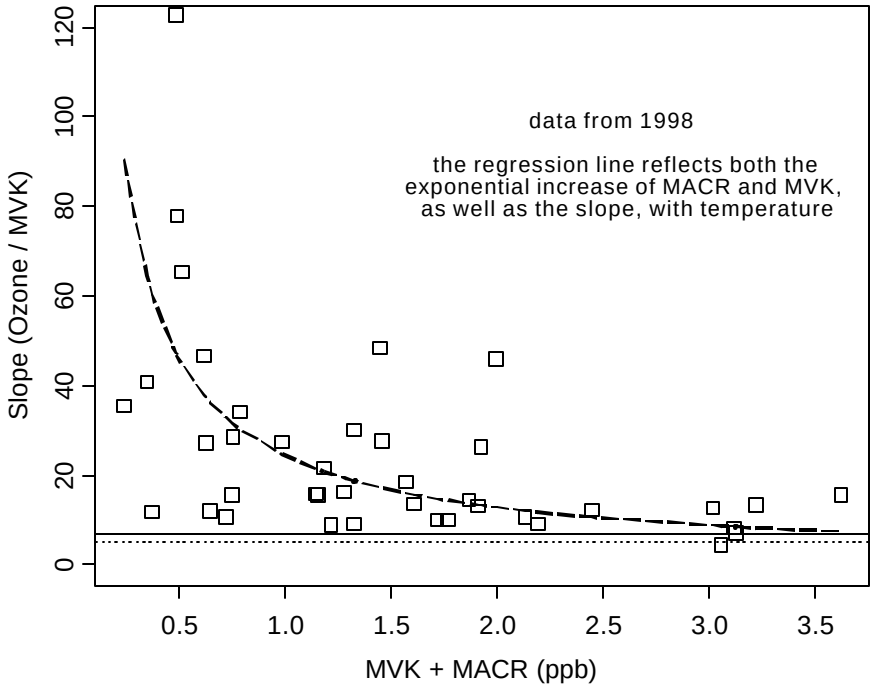

Figure 9. Daily slope of MVK versus ozone versus the sum of isoprene's oxidation products in 1998. The dotted line represents a ratio of 5 ozone per MVK, the solid line represents 7 ozone per MVK.

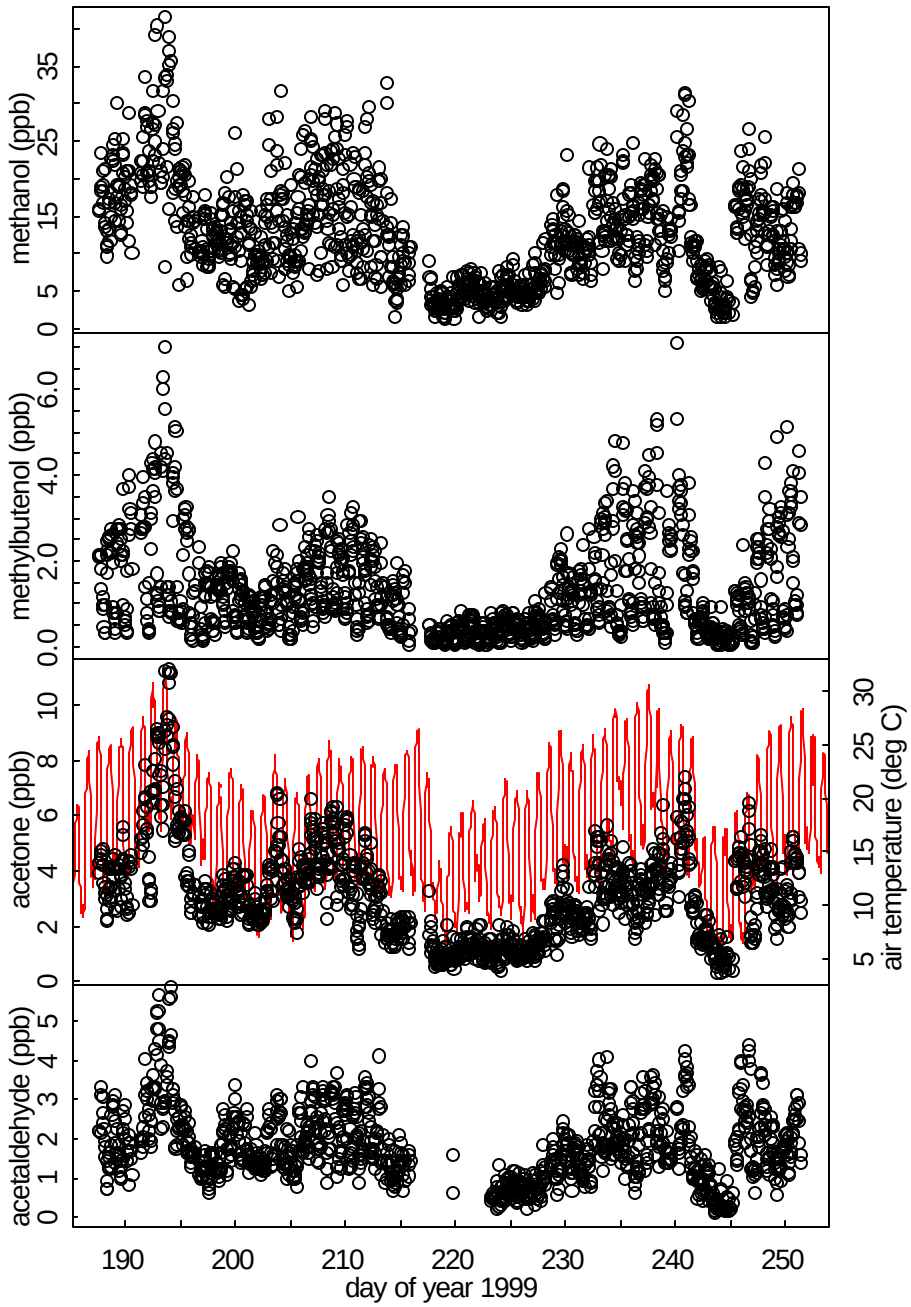

Figure 10. Mixing ratios of four OVOCs, as well as air temperature during the entire measurement period from July to September 1999 (updrafts).

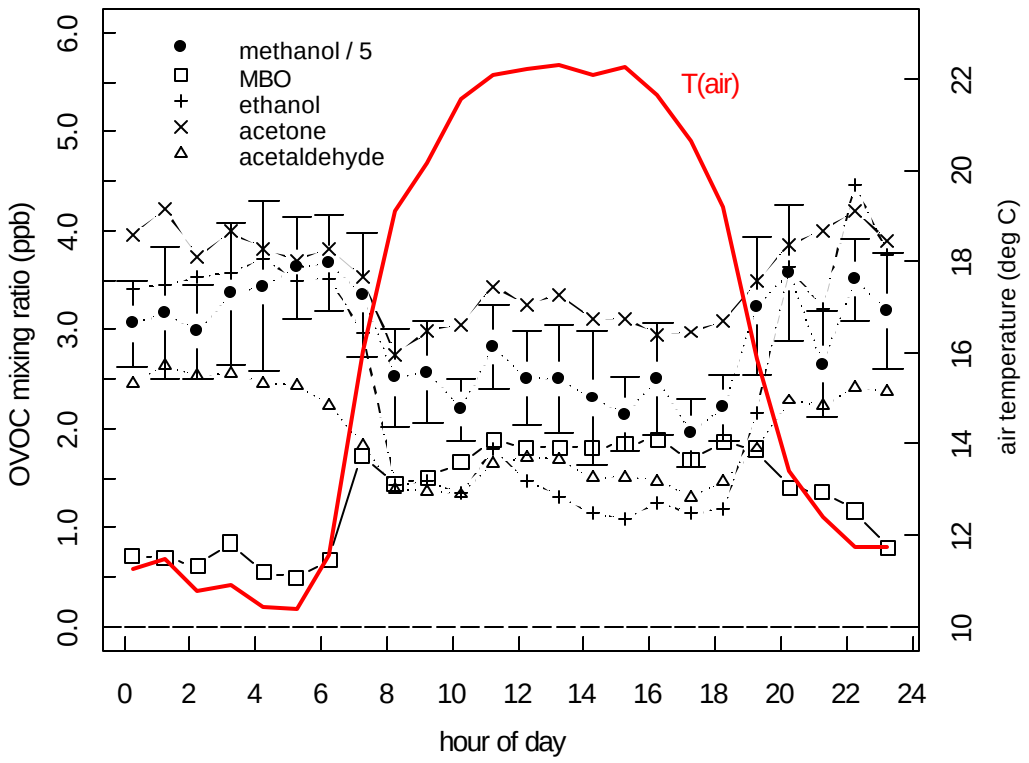

Figure 11. Mean diurnal mixing ratio cycles of five OVOCs during July 20 to August 2, 1999. Points are averages of 10-14 measurements; error bars are 90% confidence levels.

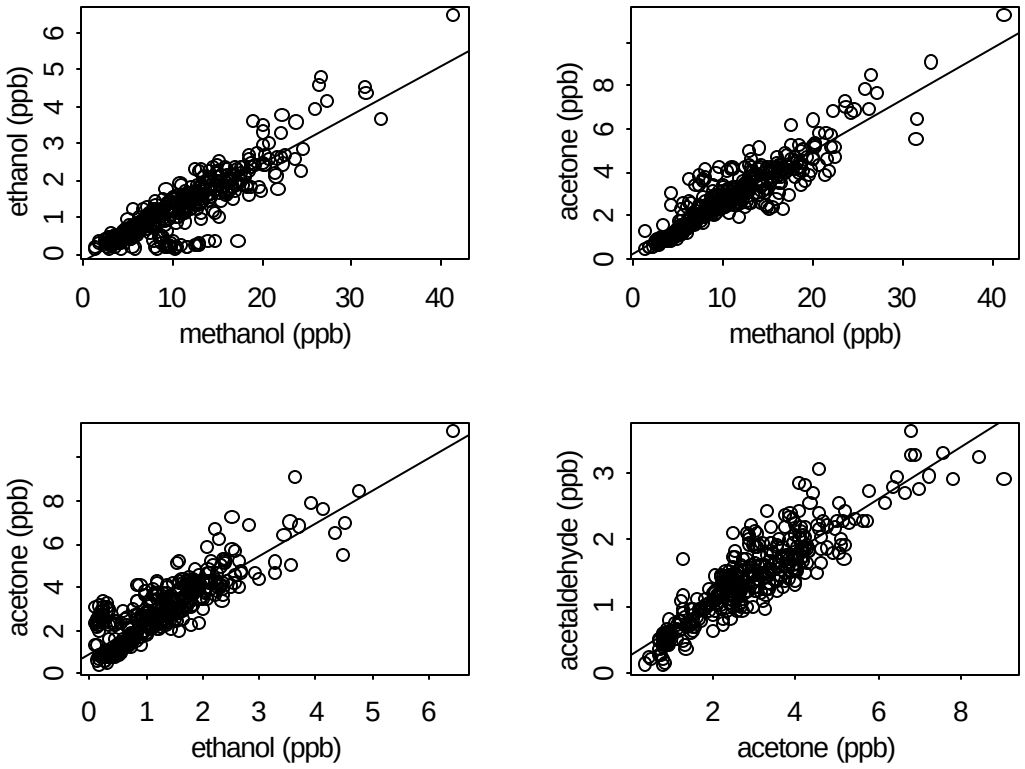

Figure 12. Daytime correlations between the OVOC mixing ratios (updrafts).

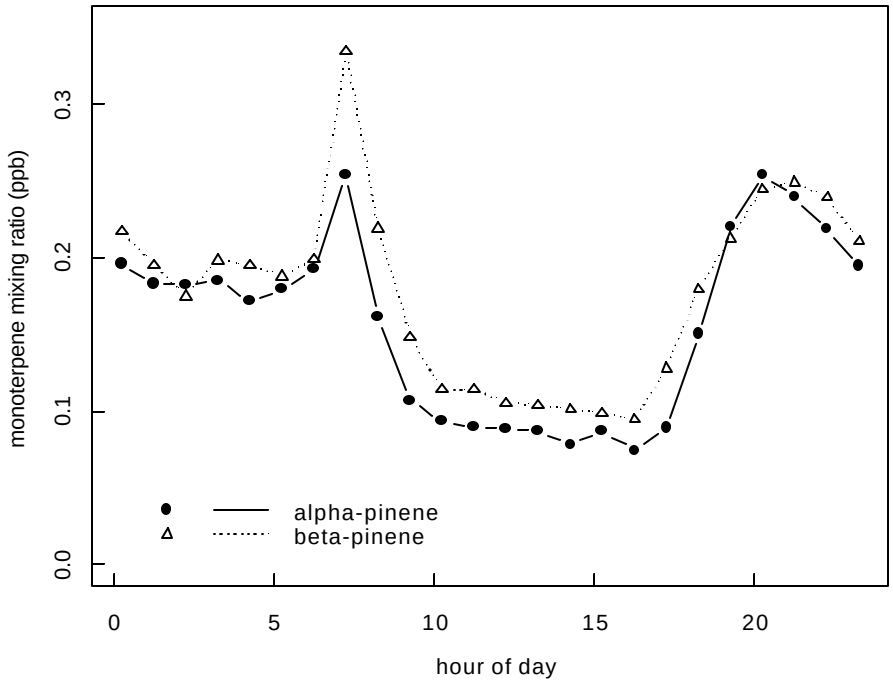

Figure 13. Mean diurnal cycle of monoterpene mixing ratios.

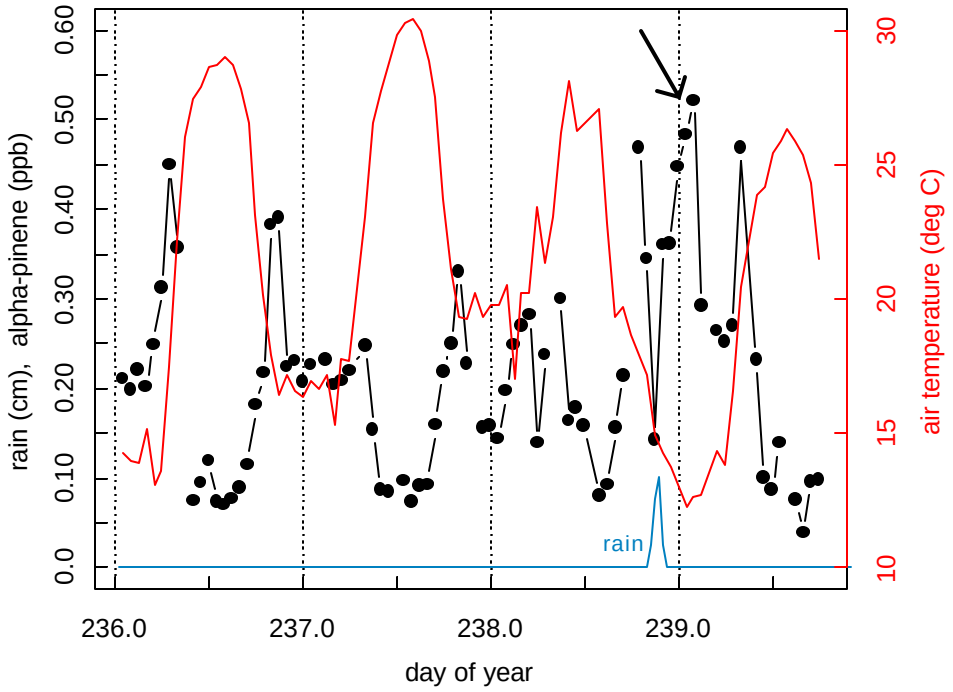

Figure 14. Impact of rain on α-pinene mixing ratios.

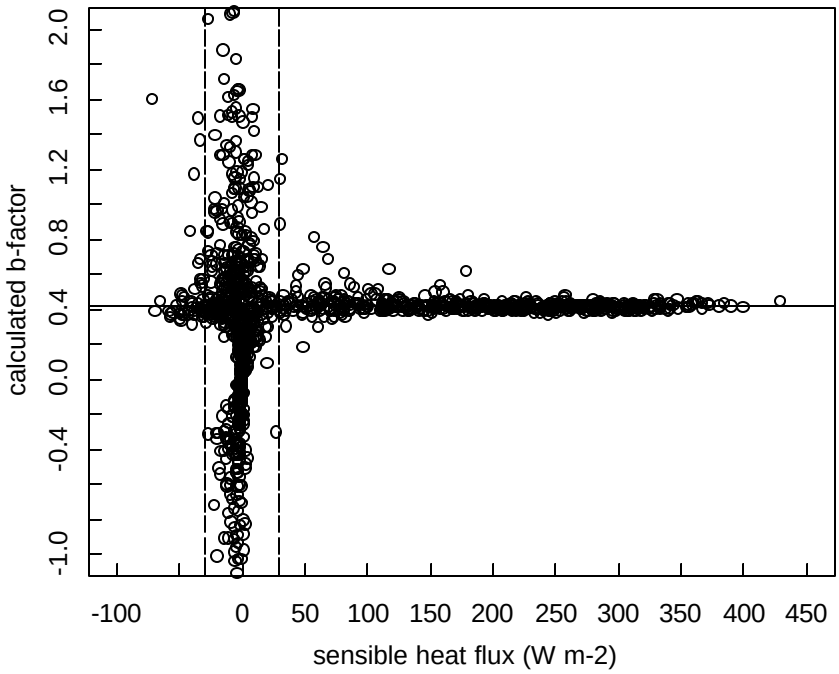

Figure 15. Variation of the calculated REA *b*-factor with sensible heat flux. The vertical dashed lines bracket the measurements for which the *b*-factor was set to its mean (horizontal solid line).

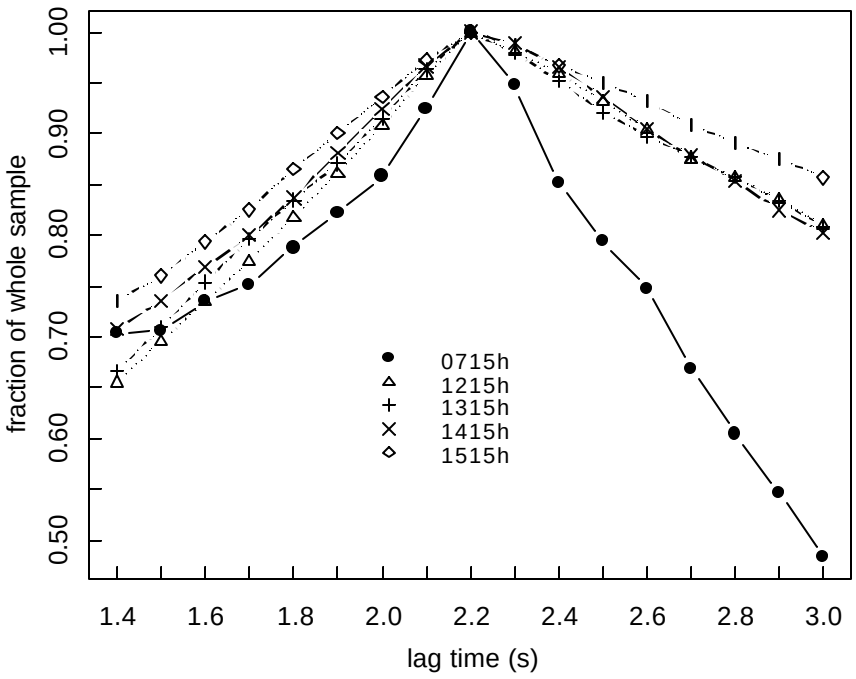

Figure 16. Theoretical variation of the *b*-factor with a changing lag-time for different times of the day. The fraction on the *y* axis corresponds to the minimum *b*-factor, which represents the maximum sampling efficiency, divided by the individual *b*-factor. Each curve represents a single 30 min measurement period.

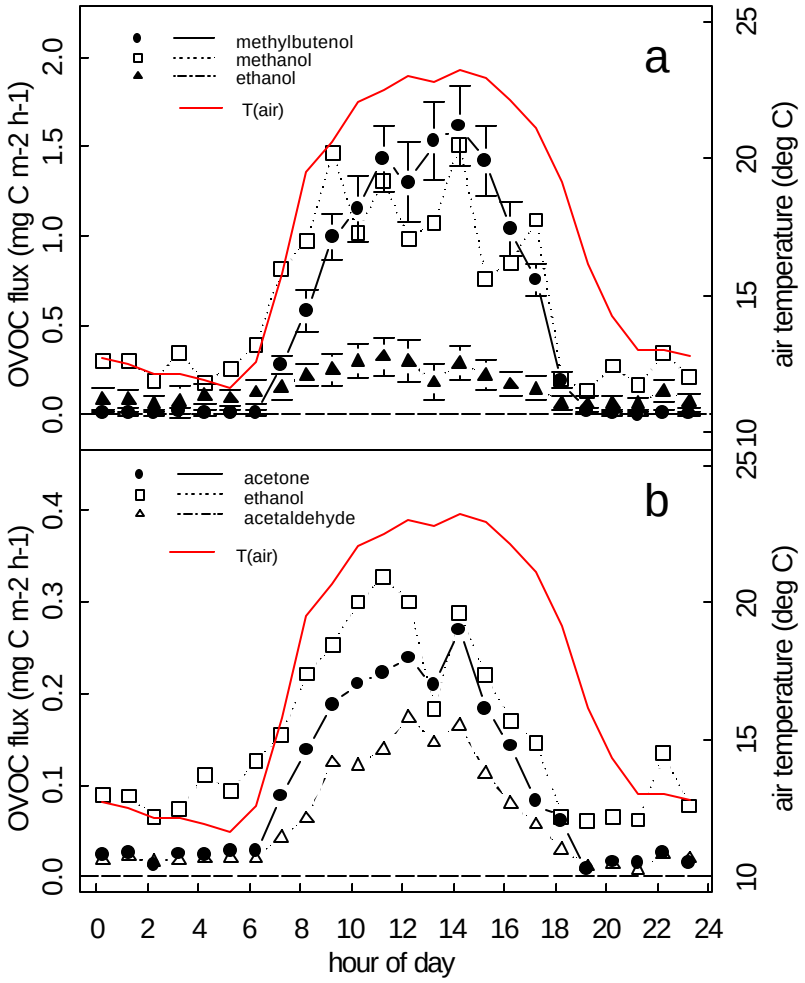

Figure 17. Diurnal variation of OVOC fluxes for (a) MBO, methanol, and ethanol, and (b) acetone, acetaldehyde, and ethanol. Error bars are 90% confidence levels.

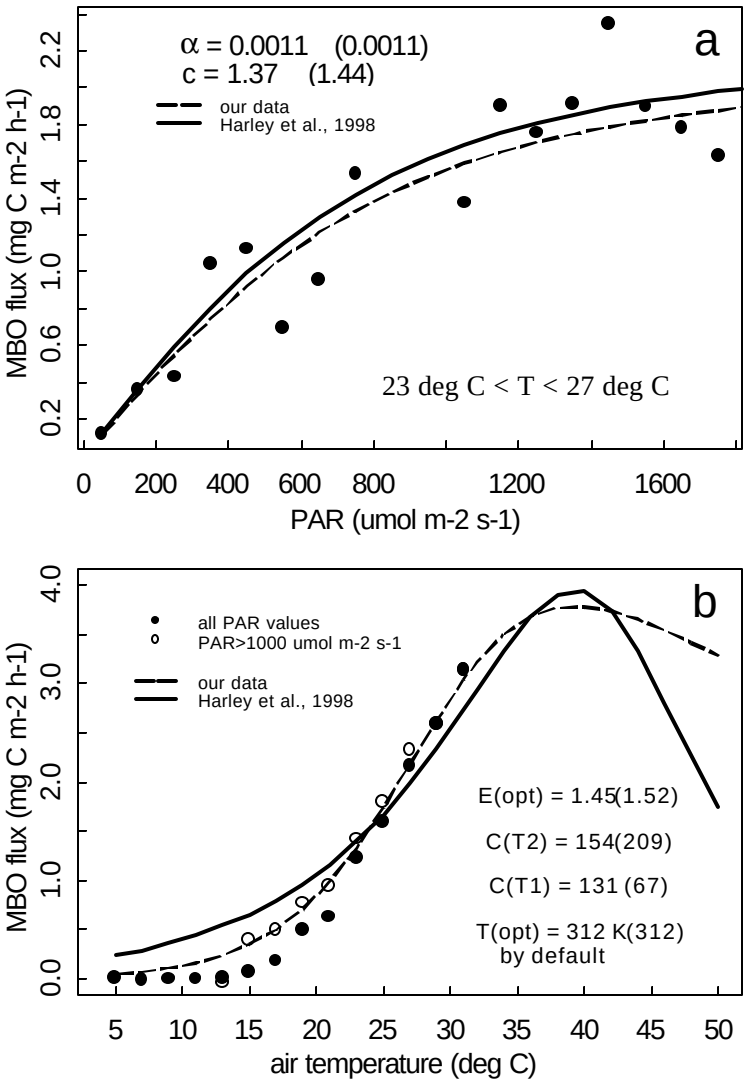

Figure 18. (a) Light and (b) temperature dependence of the measured MBO fluxes. The model equations used are $C_L = \alpha\, c\, \mathrm{PAR}\, \{1 + \alpha^2\, (\mathrm{PAR})^2\}^{-1/2}$, and $C_T = E_{opt}\, C_{T2}\, \exp(C_{T1}\, x)\, \{C_{T2} - C_{T1}\, (1 - \exp[C_{T2}\, x])\}^{-1}$, with $x = [(1/T_{opt}) - (1/T)]\, R^{-1}$, where T is temperature, R is the ideal gas constant, E_{opt} is the maximum emission capacity that occurs at T_{opt}, and C_L and C_T stand for the respective MBO emission. The numbers in parentheses next to our own model parameter calculations represent the parameters calculated from the leaf level response by *Harley et al*. [1998].

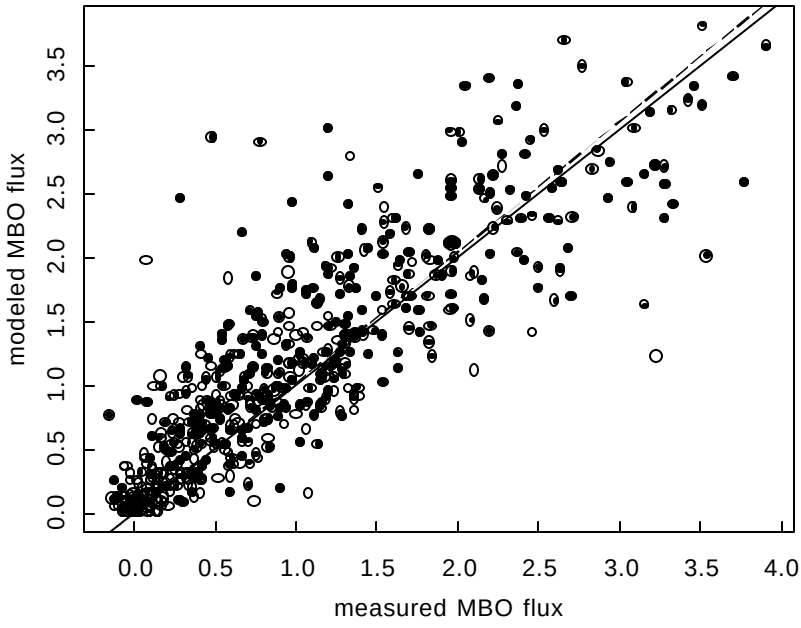

Figure 19. Measured versus modeled emissions of MBO. The dashed line shows the best fit to the main daytime values (closed symbols, hours 1000-1830), the solid is a 1:1 line.

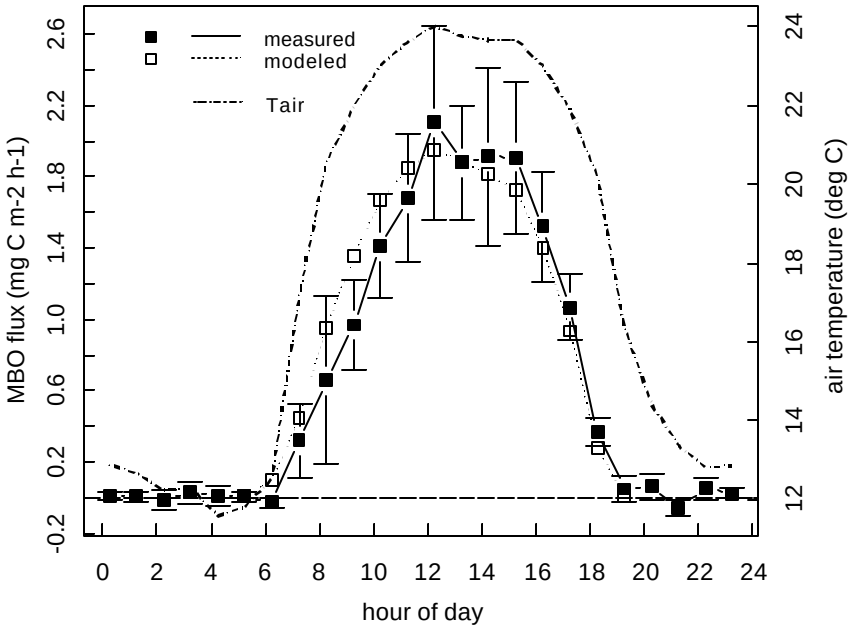

Figure 20. Diurnal changes of measured and modeled MBO fluxes, and air temperature during a representative week in late July 1999.

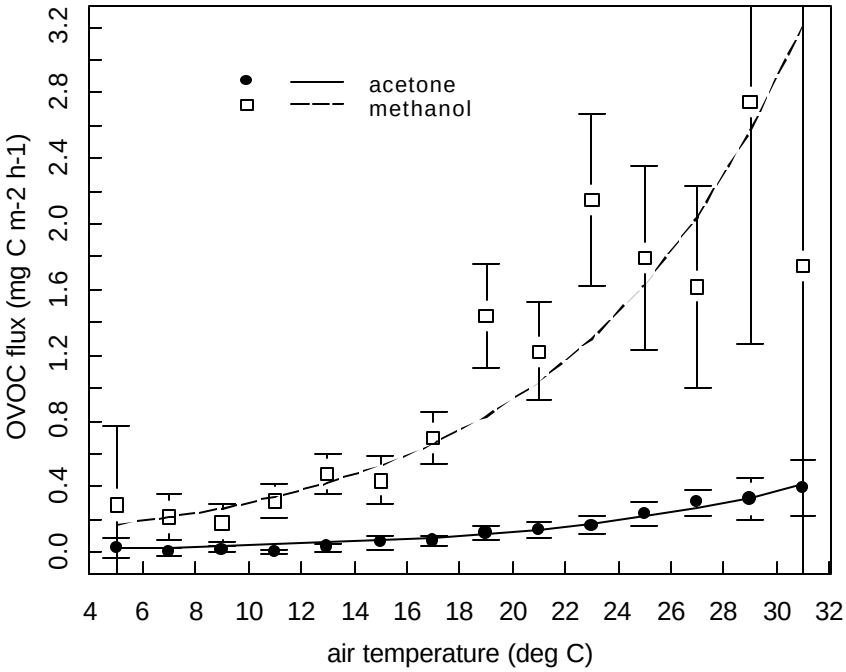

Figure 21. Temperature dependence of acetone and methanol fluxes. Error bars represent 95% confidence levels.

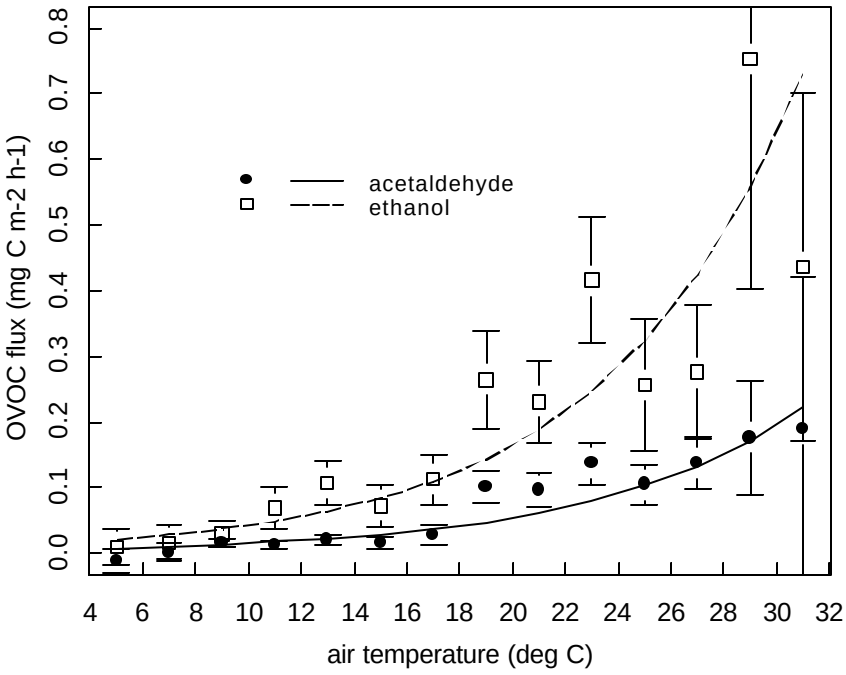

Figure 22. Temperature dependence of acetaldehyde and ethanol fluxes. Error bars represent 95% confidence levels.

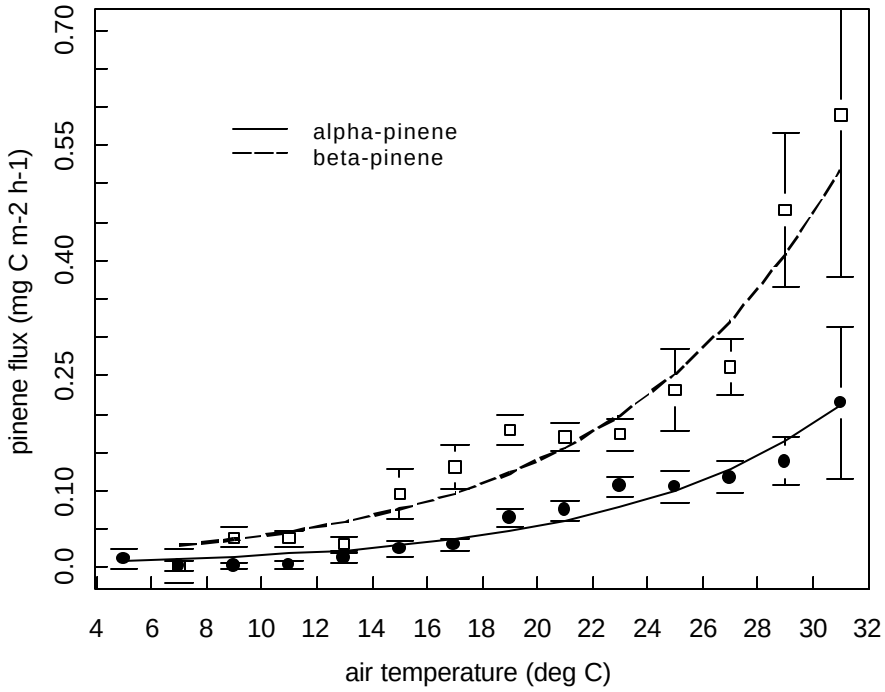

Figure 23. Temperature dependence of α- and β-pinene fluxes. Error bars represent 95% confidence levels.

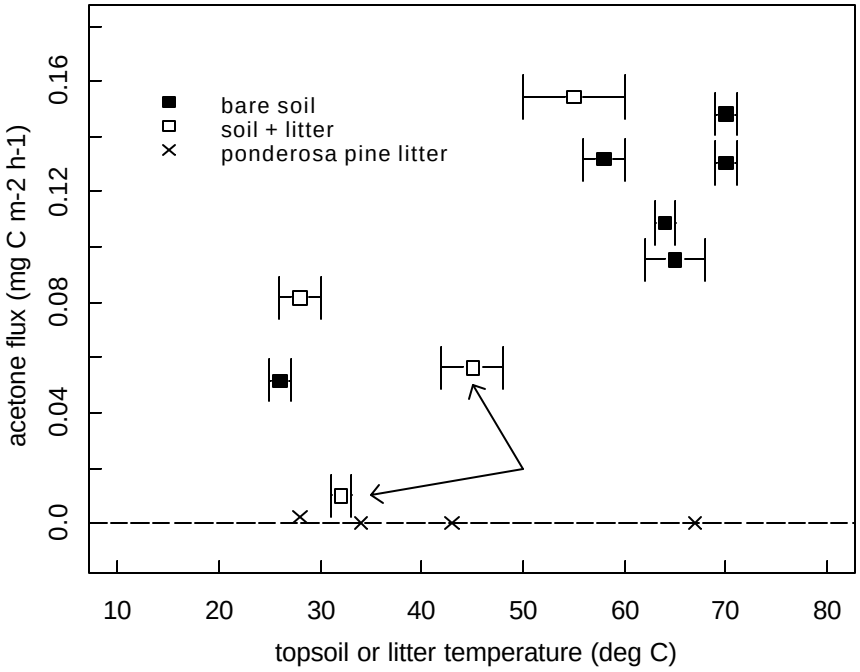

Figure 24. Acetone fluxes measured with chamber experiments. No significant acetone fluxes were measured when ponderosa pine litter alone was in the chamber, and the arrows mark the measurements where ponderosa pine litter covered the soil. The error bars represent the measured range during the half-hour sample period.

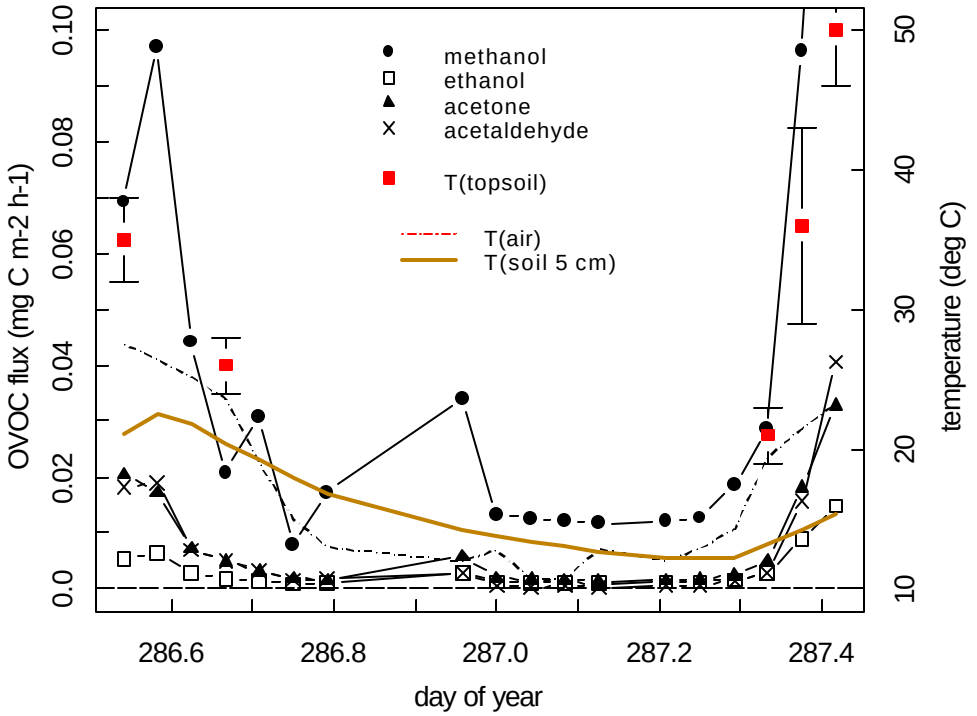

Figure 25. OVOC fluxes measured during an overnight chamber experiment from noon, October 13, to noon, October 14, 1999. Note the large difference between topsoil and soil temperatures at 5 cm depth after sunrise.

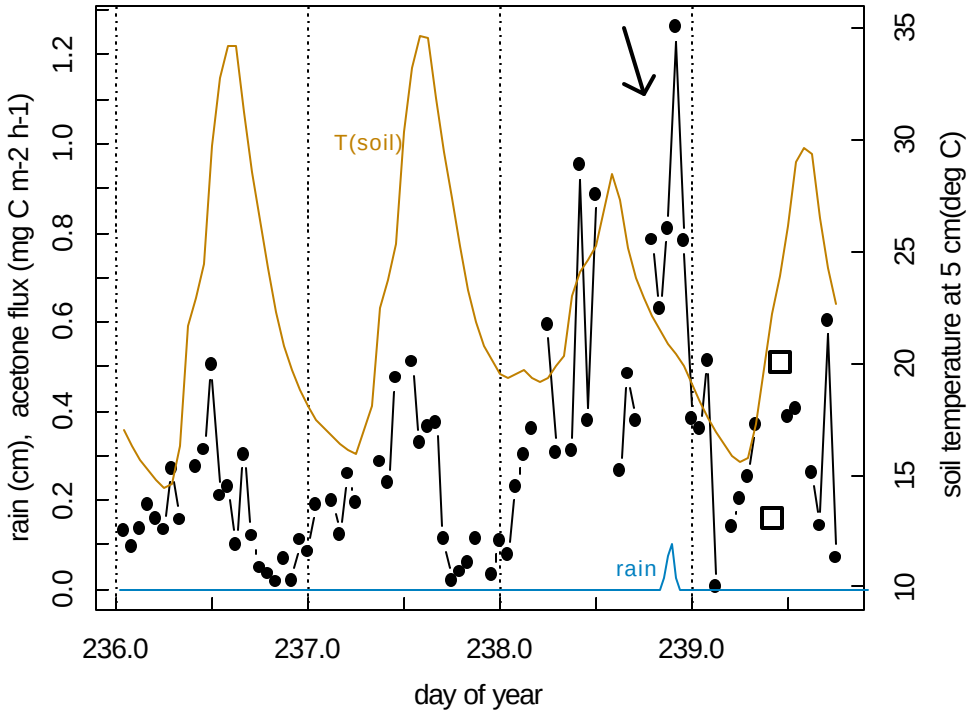

Figure 26. Canopy-scale (closed circles) and soil chamber (large open squares) acetone fluxes before and after a minor rain event during the evening of August 26, 1999 (marked by an arrow). The two soil efflux samples had topsoil temperatures of 24° and 40°C.

Appendix A: Data sets description

I. Data set **hc99_v1**:

General:

This data set contains mixing ratios of biogenic and anthropogenic volatile organic compounds measured between July 6 and September 8, 1999. All values are reported in ppb. All compounds have been identified by retention time compared to addition of standards to real air samples. It is still possible that co-elutions of other unidentified compounds could affect the reported mixing ratios or fluxes. Calibration was carried out against one or more diluted ppm-Standards as described in the text and below. All mixing ratio data are from “up-drafts”. Some very high and very low mixing ratios that were identified as outliers have been set "NA". All samples that contain standard additions have been set “NA”.

The microtraps were changed once during the measurement period. Chromatographic columns (Rtx-Wax columns, 60 m, wide-bore: 0.53 mm ID) were cut when necessary to remove degraded parts.

Note: All chromatograms have been integrated manually for proper identification and quantification. A small amount of human error, however, is of course unavoidable. Zero mixing ratios were not set "NA".

Compound description (numbering refers to column number):

(Calibration Standard(s) used for identification and quantification is(are) given in parentheses behind compound name)

0. "time": Day of year + decimal day fraction. Note that the time line is NOT based on local summer time (PDT), but on local standard time (Pacific Standard Time = PST); value is centered on the full hour.

1. "hour": Hour of measurement during that day in decimals; value is centered at 15 min after the full hour, the middle of the actual sampling interval.

Isoprene and its oxidation products:

2. "isoprene" (S1, OVOC): C_5H_8, biogenic VOC; among the most precisely measured compounds; stable response throughout the whole data set.

3. "MVK": Methyl-vinyl-ketone, C_4H_6O, major isoprene oxidation product; a small blank interference was removed from the MVK data throughout the data set, however, comparing the nighttime mixing ratios to 1998 data, we have to assume that this minor interference was not stable but may have introduced a positive bias into the nighttime MVK data, which we were unable to identify; the compound is not calibrated with an external standard, but its FID- response is assumed to equal that of MACR (see next).

4. "MACR" (S1, OVOC, BPIN): Methacrolein, C_4H_6O, major isoprene oxidation product; among the most precisely measured compounds throughout the data set. **Note**: The theoretical response factor based on the relative FID response of MACR versus isoprene was used for calibration rather than the actually measured response factors according to our standard (would have been 20% higher).

5. separation vector.

Oxygenated VOCs:

6. "methanol" (OVOC): CH_3OH, most abundant VOC; has both biogenic and anthropogenic sources and long atmospheric lifetime; mixing ratios should be viewed with some caution, as they are empirically corrected for the coeluting compounds methyl-ethyl-ketone, and 3-methyl-furan; varying occurrence in blank samples.

7. "ethanol" (OVOC): C_2H_5OH, partially coeluting with benzene; mixing ratios may slightly overestimate actual abundance; sources are dominantly biogenic; small and varying occurrence in blank samples.

8. "acetaldehyde" (OVOC): CH_3CHO, most abundant alkanal measured; has anthropogenic and biogenic sources; mixing ratios might be overestimating actual abundance due to a minor coelution with an unknown compound; small and varying occurrence in blank samples.

9. "acetone" (S1, OVOC): $(CH_3)_2CO$, most abundant ketone measured; among the most precisely measured compounds; very long atmospheric lifetime; major MBO oxidation product; no known chromatographic interferences.

10. "MBO" (MBO, BPIN): Methylbutenol, C_5H_9OH, dominant local emission compound from ponderosa pine; most abundant reactive hydrocarbon.

11. separation vector.

Monoterpenes:

12. "a-pinene" (S1, S2): α-pinene, $C_{10}H_{16}$, monoterpene; emitted from ponderosa pine and other trees in the area; no known chromatographic interferences.

13. "b-pinene" (BPIN): β-pinene, $C_{10}H_{16}$, monoterpene; emitted mostly from ponderosa pine in the area; no known chromatographic interferences; β-pinene shows issues of instability and conversion (often into another monoterpene) presumably during desorption from the microtraps, wherefore the given mixing ratios may partially be underestimates.

14. "3-carene" (S2): Δ-3-carene, $C_{10}H_{16}$, monoterpene; emitted mostly from ponderosa pine in the area; no known chromatographic interferences; Δ-3-carene shows issues of breakthrough at higher mixing ratios, wherefore the given mixing ratios may partially be underestimates, and obvious outliers have been removed from the data set.

15. separation vector

Anthropogenic VOCs:

16. "MTBE": Methyl-*tertiary*-butyl-ether, $C_5H_{12}O$; only quantified VOC of unequivocally solely anthropogenic origin; retention time identified with authentic standard; its FID response was estimated theoretically from comparison with isoprene; mixing ratios should be viewed with some caution due to incomplete separation from another, smaller anthropogenic compound, and acetaldehyde.

17. "toluene" (BPIN): anthropogenic, aromatic hydrocarbon, C_7H_8; occasional, very small blank sample; no known chromatographic interferences; no indication of biogenic sources as suggested by other authors.

Standards (manufacturer's accuracy in parenthesis):

S1 (Scott-Marrin): acetaldehyde (±5%), MACR (±10%), heptane (±2%), α-pinene (±2%), acetone (±2%), isoprene (±2%)
balance: nitrogen

S2 (Scott-Marrin): heptane, Δ-3-carene, α-pinene, d-limonene (unanalyzed Standard; α-pinene and heptane are consistent with S1).
balance: nitrogen

MBO (Scott-Marrin): 2-methyl-3-buten-2-ol (±2%)
balance: nitrogen

OVOC (Scott-Marrin; mixing ratios assigned by NCAR and highly uncertain for the aldehydes and alcohols): butane, isoprene, acetaldehyde, acetone, butanal, MACR, MEK, methanol, benzene, ethanol, pentanal, 2-pentanone, hexanal, n-butanol
balance: nitrogen

BPIN (Scott Marrin): β-pinene (±2%), MACR (±2%), MBO (±2%), toluene (±2%), 3-methyl- furan(±2%)

balance: nitrogen

II. Data set **f_hc99_v1**:

General:

This data set contains the fluxes of biogenic volatile organic compounds as calculated from equation 3, for the time period between July 6 and September 8, 1999. All flux values are reported in mg C m^{-2} hr^{-1} (carbon mass units). See text for details on calculation and error estimates. All fluxes have been scrutinized for outliers. Negative fluxes were not removed from the data set. Fluxes for MACR are not defined due to its use as channel intercomparison compound. Fluxes of isoprene and MVK were clearly within the error limits of detection, and the data suggest that, if MVK were deposited, its average deposition velocity would most probably be smaller than 0.5 cm s^{-1}, and likely smaller than 0.3 cm s^{-1}.

Compound description:

0. "time": same as described under I.

1. "hour": same as described under I.

Oxygenated VOCs:

2. "methanol": CH_3OH, data should be viewed with some caution due to the corrections applied to the mixing ratios; emissions seem to be temperature and light-driven.

3. "ethanol": C_2H_5OH; emissions appear to be mostly temperature-driven.

4. "acetaldehyde": CH_3CHO; emissions appear to be mostly temperature-driven.

5. "acetone": $(CH_3)_2CO$; emissions appear to be mostly temperature-driven.

6. "MBO": Methylbutenol, C_5H_9OH; emissions are temperature- and light-driven.

7. separation vector.

Monoterpenes:

8. "a-pinene": α-pinene, $C_{10}H_{16}$; emissions are mostly temperature-driven.

9. "b-pinene": β-pinene, $C_{10}H_{16}$; emissions are mostly temperature-driven; data after day 214 have been removed due to possible losses on one chromatographic channel that lead to an offset which could not be corrected for; mean flux data reported in Table 1 refer to a shorter and warmer time period and can therefore not directly be compared to the α-pinene and Δ-3-pinene data without restricting these to the same time period.

10. "3-carene": Δ-3-carene, $C_{10}H_{16}$; emissions are mostly temperature-driven; data between days 217 and day 233 have been removed due to losses in the chromatographic channels; mean flux data reported in Table 1 refer to shorter and warmer time periods and can therefore not directly be compared to the β-pinene or α-pinene data without restricting Δ-3-carene to the data availability of β-pinene.

III. Data set **met_hc99_v1**:

General:

This data set contains meteorological data useful to interpret the VOC data sets.

Compound description:

0. “time”: as described under I.
1. “hour”: as described under I.
2. “wind speed”: reported in m s^{-1}, measured at ~6 m above the average tree height.
3. “wind direction”: reported in degrees, measured at ~6 m above the average tree height.
4. “PAR”: photosynthetically active radiation in µmol m^{-2} s^{-1}; measured at approximately 6 m above the average tree height.
5. “rH”: relative humidity in percent: measured at the average tree height.
6. “Tair”: air temperature in degrees Celsius: measured at the average tree height.
7. “pressure”: ambient pressure in mbar measured at the average tree height.
8. “ozone”: ambient mixing ratio in ppb, measured ~6 m above the average tree height.